Mineralogy and chemistry of tellurium in the hypogene and supergene environments

USGS Award MRERP Number# USGS/G12AP20054

Principle Investigator (P. G. Spry)

S. M. Hayes[1], P. G. Spry[2], K. J. Spaleta[1], A. E. Skidmore[1], R. Witte[1], N. Knight[1], D. Knight[1], K. Milke[1]

[1] Department of Chemistry and Biochemistry, 900 Yukon Drive Rm. 194, Fairbanks, University of Alaska Fairbanks, AK 99775-6160

[2] Department of Geological and Atmospheric Sciences, 253 Science I, Iowa State University, Ames, IA 50011-3212

1. Introduction

Our society is increasingly dependent on high technology devices, which are often underpinned by scarce elements, but industrial demand often exceeds our understanding of how to explore for and recover these elements. Limited knowledge of tellurium (Te) geochemistry in ore-forming environments hinders effective exploration, accurate estimates of current resources, and efficient extraction. Uncertainties surrounding future supply and price instabilities have sparked concern amongst industries and governmental agencies around the world, leading to the creation of several lists of critical elements. Critical elements have been identified by stakeholders as elements that do not have a stable market, have low crustal abundance, are either sourced from few locations on Earth, or are recovered as byproducts [1-4].

Tellurium has been classified as a (near-) critical element due to increased use in high technology devices, historic price volatility, low average crustal abundance (~3 $\mu g\ kg^{-1}$), and is extracted as a byproduct of base metal (>90% Cu) smelting at a single location within the United States [1, 2, 5, 6]. Recent demand has grown due to unique semiconductor properties that have found application in efficient, yet inexpensive, solar panels and thermoelectric materials. An estimated near term increase of 40-100-fold current Te production is required for Te-based devices to contribute substantially to meeting growing global energy demands [7, 8]. The required gains in Te production can be made through a combination of several strategies, including mining Te as a primary ore [9, 10], improving byproduct Te recovery from current mining operations [11-13], and by streamlining manufacturing processes to use less Te [7]. **The overarching goal of this study was to examine the potential for optimization of Te byproduct recovery from operating Cu and Au mines in an effort to supply Te to emerging industries and examine surficial Te geochemistry (Fig. 1)**. The specific goals of this project were to:

1. Investigate the distribution Te between tellurides, sulfides, and sulfosalts in ores.
2. Trace Te flux and speciation through current Au and Cu extraction processes.
3. Examine mine wastes to determine the weathering trajectory and secondary phases during oxidation.

This project represents a preliminary examination of the behavior of Te throughout the Cu extraction process at ASARCO (Tucson, AZ), and Au extraction at the Golden Sunlight mine (Whitehall, MT). To that end, we established partnerships and collected samples from throughout their respective extraction processes for chemical and mineralogical analysis. Additionally, historic, Te-bearing mine tailings from Delamar, NV were examined to assess the surficial transport in a semi-arid environment as well as the fate and bioaccessibility of Te in the environment.
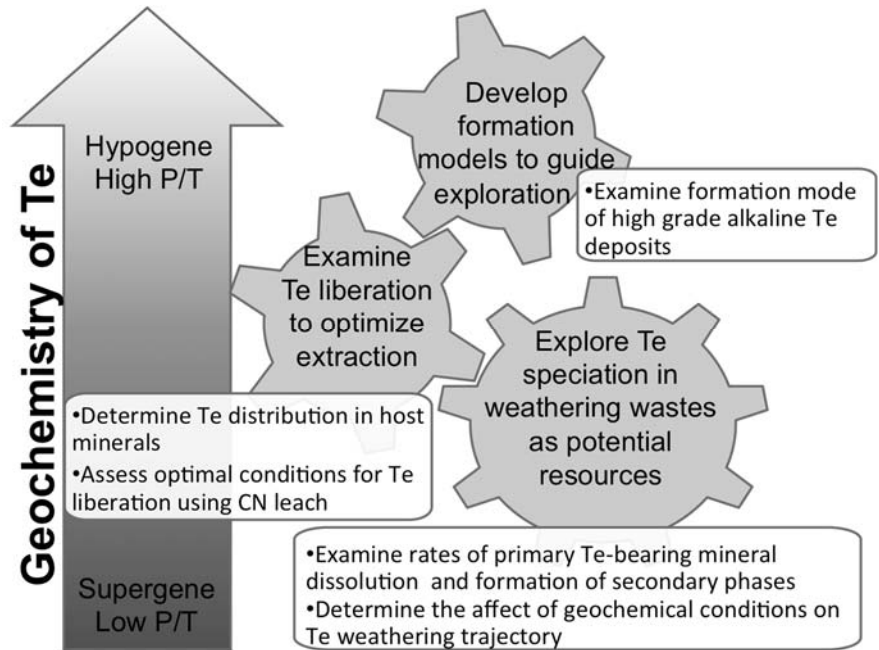
Figure 1: Goals of the study.

2. Background

Supply of energy critical elements, including Te, has garnered significant attention from the scientific community, policy makers, and popular media since 2009. This has brought into focus that the elements needed for high technology applications frequently occur at extractable concentrations in only a few identified deposits worldwide, leaving industry in the United States vulnerable to price volatility and supply shortages when/if unfriendly governments control the supply of these elements [14]. Concerns of future supply are enhanced because of limited knowledge of Te geochemistry, which hinders effective exploration, accurate estimates of current resources, and efficient extraction strategies.

Tellurium, used in highly efficient photovoltaics and thermoelectrics, is classified as an energy critical element because of rarity (crustal abundance 3 $\mu g\ kg^{-1}$), and recent price volatility due to changes in the Te market during the last decade [5, 6]. Currently, Te is recovered almost exclusively as a byproduct of Cu mining, but significant potential resources exist in high-grade Au-Ag telluride deposits across the western United States [5]. Small improvements in Te recovery would mean substantially more Te could be made available to emerging technology industries. The few studies that have examined Te recovery from Cu extraction report very low overall (~2%) recoveries [11, 13], but none have linked recovery to the distribution of Te between host minerals (e.g., telluride minerals, substitution into sulfide minerals, sulfosalts, and elemental Te).

Currently, Te is of little economic consequence in the Au or Cu mining industries, and no Te is recovered from Au mining. Improving or initiating Te recovery hinges on knowledge of Te mineralogy, speciation, and behavior in current extraction processes, which is the goal of the current study. Further, extracting Te would limit the amount of Te reaching surficial waste piles. Little is known about Te behavior in the surficial environment or potential toxic effects on nearby communities and ecosystems, but the

few studies performed challenge the common assumption that Te behaves in a similar way to Se in the environment [15], highlighting the need for direct observations.

2.1. Uses of tellurium

The last ten years has seen significant changes in the end uses of Te with emerging applications in high technology devices capitalizing on the semiconductor properties of this metalloid. Between 2001 and 2013, the percentage of Te used in semiconductor applications increased from <15% to >70%, which was accompanied by dramatic price fluctuations from $10 kg^{-1} in 2001 to over $360 kg^{-1} in 2011 [5]. The price in January, 2015 of ~$125 kg^{-1} is considered low relative to other commodity elements with low crustal abundance [2]. Growing industrial use of Te is in high technology applications (40% for photovoltaics and 30% in thermoelectrics) has been hampered by a lack of abundant, inexpensive Te supply, and has also contributed to the decline of Te use in other industries [5, 8]. Other uses of Te include as an additive to steel and Cu to improve machining properties (15%), as a vulcanizing agent and accelerator in rubber processing (5%), and in a variety of other applications (10%). A consistent, inexpensive Te resource is key to continued growth of Te-based alternative energy industries.

Photovoltaic devices convert photons to an electrical current within semiconductors and are the basis of solar panels [16]. This industry is the single largest industrial Te consumer and CdTe-based solar panels are inexpensive to manufacture ($0.84 W^{-1}) and have efficiencies approaching those of the most efficient crystalline silicon cells (25.6%), up to 17% whole panel and 21.7% in research cells [7, 16, 17]. About 266 tons of Te are required to produce one gigawatt power [9].

Thermoelectric devices are used in refrigeration and portable power generation based on making a temperature difference when a voltage is applied or creation of a voltage from differences in temperature [18]. Lead and bismuth tellurides are excellent thermoelectric materials that have been used extensively [19-21]. Lead telluride (PbTe) has a high melting point, good chemical stability, low vapor pressure, and good chemical strength and, when doped with PbI_2, is a well-known n-type thermoelectric material for 50-600 °C with variable thermoelectric properties [20, 22-24]. Bismuth telluride (Bi_2Te_3 or as naturally occurring tellurobismuthite) has also been studied extensively and is one of the most widely used thermoelectric materials [19, 21].

2.2. Potential tellurium resources

Uncertainties over Te supply highlight the importance of a more detailed understanding of Te behavior in ore-deposits and under extraction conditions [1]. Assessment of the future of Te supplies requires accurate assessment of the quantity of extractable Te available as well as the cost of transformation to industrially relevant forms. A key component in this is an increased understanding of Te behavior and mineralogy under ore-forming and extraction conditions. Over 90% of Te worldwide is recovered from anode slimes, a byproduct of Cu extraction, with the remainder contributed by sludges produced from Pb refining, about ~450 t Te yr^{-1} is recovered globally [6]. It is estimated that Te production could be readily increased to 1,200 t Te yr$^-$

[1] by improving Te recovery from current operations [2, 6, 11]. Tellurium is recovered only from pyrometallurgical refining of porphyry copper deposits, and is not recovered from ores treated by heap leaching. Additional Te could be recovered by several strategies, including mining the few deposits warranting Te extraction as a primary ore and initiating Te byproduct or co-recovery from current mining processes [7, 9, 10]. Alternatively, decreasing the amount of Te needed during the manufacturing process can also stretch Te resources [7].

Unfortunately, there are very few locations worldwide where Te can be economically mined directly, which requires concentrations of 1% Te by weight [9]. These deposits include the Moctezuma deposit in Sonora, Mexico, and the Dashiougou deposit, China, where Te was or is recovered as a co-product along with Au and Bi [9, 25]. Although not widely exploited world-wide, tellurium locally occurs in Au-Ag telluride deposits in concentrations that could be economically recovered. Tellurium was once extracted as a byproduct of gold mining at, for example, the Emperor gold mine, Fiji [12, 26]. Active plans to recover Te are ongoing at several other locations, including by Boliden Mineral AB at the Kankberg Zn-Cu-Au-Te deposit, Sweden (3.5Mt @ 4 ppm Au and 160 ppm Te) [27].

2.3. Tellurium-bearing ore types

Tellurium-bearing minerals have been described from many deposits, however there have been few specific geologic models developed on how Te-enriched deposits form or how to explore for them [e.g., [28, 29]]. The resource potential for Te deposits in the United States depends upon the economic potential of gold-silver or porphyry copper mineralization [30, 31]. Tellurium is associated in trace amounts with mainly porphyry and epithermal deposits, however detailed mineralogy is required to determine the mineral associations of Te in order to be able to design appropriate mineral processing and extraction methods.

Porphyry copper (±molybdenum±gold) deposits are large, low-grade (<0.8% Cu) deposits that contain disseminated, breccias and stockwork veinlets of copper sulfides (±molybdenite) associated with porphyritic intrusive rocks [e.g., [32-34]]. These copper deposits are typically found in and around relatively small porphyritic diorite, granodiorite, and quartz monzonite stocks that were intruded at relatively high crustal levels, commonly within 1-6 km of the surface, and are surrounded by concentric zones of hydrothermal alteration [34]. Magmatic-hydrothermal solutions are released through these fractures and react with the host rocks, altering them in a characteristic zonation pattern. Tellurium concentrations in porphyry copper deposits can be as high as 6,000 mg Te kg^{-1} (**Table 1**), but are highly variable and typically less than 1 mg Te kg^{-1}. However they are several orders of magnitude higher than the average igneous rock value of 3 μg Te kg^{-1} [33]. For example, analyses of 372 samples of jasperoids and gossanous rocks in the central part of the Ely porphyry copper district contain up to 66 μg Te kg^{-1}, which Gott and McCarthy suggested would make it the largest resource of Te in the United States [35].

It should also be noted that epithermal vein- and skarn-type mineralization are also spatially associated with the porphyry-style mineralization. Au-Ag-Te veins in alkaline to subalkaline igneous rocks, which, in places, contain high-grade zones of precious metal tellurides were not evaluated here [27, 28, 39, 40, 53]. High- and low-sulfidation epithermal vein deposits are spatially associated with porphyry Cu/Mo mineralization in various locations and may either form distal to the copper mineralization or telescoped onto the copper mineralization. These veins generally form at lower temperatures (150 to 300 °C) after the high-temperature (~ >350-700°C) copper mineralization formed. Low-grade porphyry Mo mineralization at the Golden Sunlight deposit, Montana, is spatially associated with epithermal gold-telluride veins along the margins of a breccia pipe [41, 84, 89, 94]. Tellurium in epithermal deposits is usually associated with gold and silver, often in high tenor veins/veinlets. These include, for example, the small but high-grade Mayflower and Gies Au-Ag-Te vein deposits, Montana [42, 43]

Table 1: Ranges in concentration of tellurium in selected deposits [30, 31, 33].

Type of deposit	Te (mg kg^{-1})
Gold-quartz veins	0.2-2,200
Gold skarn deposits	0.2-0.5
Polymetallic gold deposits	0.2-10
Gold quartz-pebble conglomerate deposits	<0.2-0.7
Carlin-type deposits	<0.2-0.6
Porphyry copper deposits	<0.1-6,000
Lead-zinc ores	0.5-1.0

Skarns/carbonate-hosted deposits of copper and other metals can form near the contact between intrusions and adjacent limestone, and other carbonate-bearing rocks. Skarn is a term used for rocks that can have diverse origins, but similar mineralogy, typically calcium-bearing varieties of garnet and pyroxene [36-38]. Whereas these types of deposits form in a variety of geological environments, they are common in the southwestern U.S. in contact with metamorphic deposits proximal to porphyry Cu-style mineralization [37]. Hydrothermal fluids exsolved from the igneous rocks metasomatized the calcareous wall rocks, converting them to pyroxene and garnet. Magnetite and calc-silicate minerals are also present, especially in dolomitic host rocks.

2.4. Tellurium mineralogy in ore

Tellurium in ore is principally found as tellurides or substituted into sulfides, or, more rarely, in sulfosalts and as the native element [39-43]. Tellurium is one of the few elements that can form a variety of minerals with gold as a principal component (**Table 2**). These minerals occur in many deposits such as Cripple Creek (Colorado), Emperor (Fiji), and Săcărîmb (Romania). Trace elements, including Te, can also occur in solid solution and/or as metal nanoparticles in sulfides, e.g., [44]. Pyrite in sediment-hosted gold deposits (Sukhoi Log, Bendigo, and Spanish Mountain) contain up to 12 mg Te kg^{-1} , e.g., [45], whereas up to 9 mg Te kg^{-1} Te occurs in pyrite in the orogenic Golden Ridge gold deposit, Australia [46]. Pals et al. reported ~1,000 mg Te kg^{-1} Te in solid-solution in high As-Au bearing fine-grained (framboidal) pyrite from the epithermal Emperor Au-Te deposit, Fiji, in addition to the presence of gold-telluride nanoparticles [47, 48].

6

Tellurides have been documented from several porphyry copper deposits where they occur mainly as inclusions in sulfides (e.g., chalcopyrite, pyrite, and bornite at Etastite, Bulgaria [50]; galena, and sphalerite at Bulawan, Philippines [51], chalcopyrite and bornite at Skouries, Greece [52]. However, it should be noted that there are several epithermal telluride vein systems that were superimposed on porphyry copper mineralization (e.g., Emperor, Fiji [48, 53]; Fakos, Greece [54]; Pagoni Rachi, Greece [55]; Tuvatu [40]). In most of these examples, there are primary tellurides in the porphyry copper mineralization, but the proportion of tellurides in the epithermal mineralization is generally much higher. LA-ICP-MS studies of individual sulfides in ore deposits are very limited in number. However, recently, Yano analyzed a suite of selected trace element concentrations of the sulfides in porphyry copper, skarn, iron oxide-copper-gold, and massive sulfide deposits [56]. Sample selection for LA-ICP-MS analysis was based on elevated concentrations of trace elements in bulk-rock samples of ore. Yano obtained data for one or two samples from the Bingham Canyon (Utah), Chuquicamata (Chile), Yerington (Nevada), La Colorada deposit (Mexico), and Grasberg (Indonesia) porphyry copper deposits [56]. Observed Te concentrations ranged from 0-220 ppm (32 mean) in spot analysis hosted as inclusions in chalcopyrite, bornite, chalcocite, enargite, sphalerite, and tetrahedrite. In 17 samples, Te concentrations ranged from 0.09 to 17 mg Te kg^{-1} (mean =

Table 2: Mineral names and formulas [49]	
Mineral	**formula**
Tellurides	
calaverite	$AuTe_2$
krennerite	$(Au,Ag)_2Te_2$
petzite	Ag_3AuTe_2
sylvanite	$(Au,Ag)_2Te_4$
hessite	Ag_2Te
empressite	$AgTe$
stuetzite	Ag_7Te_4
altaite	$PbTe$
melonite	$NiTe_2$
coloradoite	$HgTe$
buckhornite	$AuPb_2BiTe_2S_3$
tetradymite	Bi_2Te_2S
tellurobismuthite	Bi_2Te_3
Sulfides	
pyrite	FeS_2
chalcopyrite	$CuFeS_2$
covellite	CuS
chalcocite	Cu_2S
cubanite	$CuFe_2S_3$
bornite	Cu_5FeS_4
galena	PbS
sphalerite	ZnS
molybdenite	MoS_2
Native Te (Te^0)	
Sulfosalts Tetrahedrite group, generally: $[(Cu,Ag)_6(Cu, Fe, Zn, Hg, Cd)_6(Te,As, Bi,Sb)_4(S,Se)_{13}$	
goldfieldite	$Cu_{12}(Te,Sb,As)_4S_{13}$
tetrahedrite	$Cu_{12}Sb_4S_{13}$
tennantite	$Cu_{12}As_4S_{13}$

4.7 mg Te kg^{-1}) in chalcopyrite ($CuFeS_2$), pyrite (FeS_2), chalcocite (CuS), and tennantite ($Cu_{12}As_4S_{13}$) [56]. The last mineral contained up to 220 mg Te kg^{-1} but this is hardly surprising since tellurian tennantite, with several percent Te is known from various ore deposits (e.g., Besshi-type massive sulfide deposits, Japan [57]), and because it can form a solid solution with goldfieldite ($Cu_{12}Te_4S_{13}$), which is the Te equivalent of tennantite. The common association of elevated Te concentrations with Au, Ag, Pb, or Bi suggested to Yano that Te occurs dominantly as nanoparticles of tellurides in the lattice of sulfides rather than structurally bound in the host sulfide [56]. He also suggested that Te concentrations were higher in chalcopyrite than in pyrite, which are by far the two most

common sulfides in porphyry copper deposits. Up to 69 mg Te kg^{-1} (obtained by SIMS analysis) was reported in pyrite from the giant Dexing porphyry copper deposit, China [58]. However, Reich et al. did not specifically identify whether the Te was structurally bound in pyrite or occurred as telluride nanoparticles [58]. Tellurium mineralogical distribution within the ore will directly control behavior during extraction of primary elements of interest and eventual fate of Te.

2.5 Copper smelting process for tellurium recovery

Few studies have estimated the recovery of Te through the entire pyrometallurgical Cu extraction process. Estimates of overall recovery vary from 1.8% [13] to 4.5% [11], but both studies report an 85-90% loss of Te during the flotation step. Flotation conditions required for concentration of Cu-bearing sulfides (e.g., chalcopyrite, chalcocite) are also expected to float some fraction of other sulfides (e.g., pyrite, galena, sphalerite, molybdenite) and Au-Ag tellurides [59]. However, these studies have not directly examined the mineralogy of Te in the ore or at other stages during extraction to directly assess the reasons for poor Te recovery during the flotation process.

Relatively few studies have examined the mineralogy of Te, which is generally limited by the low concentration of Te in copper ores, generally less than 100 μg kg^{-1} [11]. Tellurium principally occurs in ores as tellurides, substituted into sulfides, or, more rarely, in sulfosalts and native Te [39-43]. Tellurides have been documented from several porphyry copper deposits where they occur mainly as inclusions in sulfides (e.g., chalcopyrite, pyrite, bornite, galena, and sphalerite) [48, 52-55], but also occur as primary tellurides with a higher proportion of tellurides in examples of epithermal mineralization [40, 50, 51]. There has been little work to examine the behavior of tellurides during Cu concentration, but some studies indicate Au and Ag tellurides should float with the Cu concentrate [59]

The smelting process involves heating ore to the point of melting so that residual gangue minerals, mostly pyrite, can be removed. The smelting process occurs in three 1200-1250 °C furnaces, the blast furnace, the converter furnace, and the anode furnace. First, the flash furnace, operates at 1200 °C and melts the Cu-rich concentrate in an oxidizing environment with the addition of silica. This generates a silicate slag phase with much of the iron from chalcopyrite and pyrite impurities as well as any residual silicates. Also in this step, some of the sulfur is oxidized to SO$_2$ (g). The converter furnace removes remaining SO$_2$ gas and the anode furnace removes oxygen and produces anode copper, which is sent to the refinery.

The anode slimes, the waste product remaining after electrorefining of copper, contains essentially all of the Te from the copper anodes. Tellurium occurs at concentrations up to 4% by mass in the slimes as tellurides Ag(Se, Te), Cu(Se, Te), or Cu$_3$(Se, Te)$_2$ [59, 60]. Chen and Dutrizac performed an extensive study of tellurium behavior during electrorefining of copper [61-64]. Three forms of Te occur in copper anodes:
1. In solid solution with copper (3-10% of Te);
2. Incorporated into oxide phases with Cu, Pb, A, Sb, and Bi (~4% of Te);
3. Telluride minerals, the most common of which is Cu$_2$(Se,Te).

Virtually all the Te in the copper anode reports to the anode slime with less than 0.1 mg Te kg^{-1} present in cathode copper resulting from entrapment of anode slime particulates [63]. During the electrorefining process, some telluride particles react with dissolved silver and oxygen to form Ag(Se, Te), Cu(Se, Te), or Cu$_3$(Se, Te)$_2$. Tellurium in solid solution with copper or associated with oxide phases is released when parent phases dissolve. This liberated tellurium can become associated as tellurite (Te^{4+}) with a variety of phases, including substitution into CuO$_2$ as Cu$_{2-4x}$Te$_x$O, Cu$_2$TeO$_3$, (Cu, Ag, Pb) TeO$_3$ •nH$_2$O or a complex oxidate phase containing Cu, Pb, Ag, Au sulfate, arsenate, antimonite, selenite, tellurite. The tellurate (Te^{6+}) PbTeO$_4$ has also been reported.

2.6 Tellurium toxicity and transformations in surficial environments

Regardless of the distribution of Te between telluride, sulfide, native Te, and sulfosalt minerals, the vast majority of the Te found in ores ends up in mining waste materials, which are deposited in the surficial environment. The minerals found in the mine wastes will undergo oxidative weathering, which can mobilize elements and alter bioaccessibility. Primary Te-bearing phases in these mine wastes are expected weather to form tellurite (Te^{IV}O$_3$$^{2-}$) or tellurate (Te^{VI}O$_4$$^{2-}$) oxyanions, depending on environmental conditions. However, disagreement exists in the thermodynamic constants for Te between datasets, results in differences in the dominant oxidation state of Te predicted under surficial conditions [65-67], and there have been very few direct measurements of Te in the surficial environments [15]. Regardless, studies have demonstrated that tellurite (Te^{IV}) is more toxic than better-known elements of environmental concern, arsenite (As^{III}) and selenite (Se^{IV}), and about 10x more toxic than tellurate (Te^{VI}) [67].

It is often assumed that environmentally released Te will behave similarly to selenium and other group 16 elements. Within the context of semi-arid systems, such as the system under study, mineral weathering liberates ions (including toxic metalloids), which are frequently translocated upward in soil profiles by capillary action and precipitated at the surface as efflorescent salts, which are characterized by small particle size and high bioaccessibility [68, 69]. Mine tailings, and other contaminated sites, frequently lack vegetative cover that acts to reduce erosion by decreasing wind speed and increase geomedia stability at the ground surface. Especially at semi-arid sites, metal(loid) particles from these disturbed, and inherent vulnerable environments, can be dispersed locally by aeolian transport [68-71], although regional and even global transport has been reported [72]. Although aeolian transport often dominates in semi-arid environments, fluvial transport during monsoon events is also important [73].

Metal(loid) toxicity depends directly on exposure route, form or speciation, and exposure dose. Tellurium toxicity has been studied in a variety of animal models [67 and references therein], and humans [74]. Animal and human studies indicate that roughly 25% of orally administered Te-oxyanions are absorbed in the gastrointestinal tract [67, 74]. Physiologically-based extraction tests (PBETs) supplement expensive animal model studies by mimicking conditions inside the gastrointestinal tract and alveolar macrophages to assess metal(loid) bioaccessibility in geomedia [75, 76]. Particles less than 40 μm are considered readily wind transportable while particles of less than 4 μm are capable of being deeply inhaled into lungs, where particles may become trapped for

months to years [75].Taken together, the potential toxicity combine with the lack of studies reporting direct observation of Te speciation in the surficial environment and high erosion potential of historic mine tailings highlights the importance of understanding the potential environmental and human health implications of Te-bearing geomedia in the surficial environment.

2.7 X-ray absorption spectroscopy

X-ray absorption spectroscopy (XAS) is an excellent tool for direct, molecular-scale investigation of Te solid phase speciation, since it is an element specific probe, sensitive to both oxidation state and atomic-scale bonding environment. The near edge or XANES region can be used to differentiate between Te oxidation state, including Te^{IV} and Te^{VI}, using the energy of edge features at both the K- and L_{III}-edges (31,814 and 4, 341 eV, respectively) [e.g., [77, 78], whereas the post-edge or EXAFS region can be used to determine the coordination number and bond distances of nearest neighbor atoms [66]. Most studies employing Te XAS have focused on industrially relevant species, but several studies have applied XAS to examining Te sorption complexes [15, 77] and Te-bearing minerals [66, 78].

Te transport in the hypogene environment, a knowledge gap that currently hinders Te exploration and controls the Te mineralogy in ores processed at ASARCO and Golden Sunlight, have been addressed using XAS. Tellurium can be transported in the vapor and liquid phases under ore-forming conditions [78]. XAS has previously been used to experimentally establish the stability of polytellurides in simulated hydrothermal solutions up to 599°C and 800 bar [79].

The behavior of Te in a surficial environment can also be probed using XAS. The sorption studies have demonstrated Te oxyanions have a strong affinity for Fe^{III} (oxy)hydroxides and bind via inner an sphere mechanism [15, 77]. One of these recent studies demonstrated divergent behavior between Se and Te in some surficial environments. However, the same study also reported Te behavior similar to Se in saturated soils, such as those encountered in wetlands [15]. Thus, the behavior of Te in a variety of environmentally-relevant conditions merits additional research to assess the environmental impacts of Te contamination.

2.8 Goals of current study

Tellurium geochemistry has received relatively little attention, but is a growing area of research as a result of recent growth in industrial demand for the rare element as well as its potential for deleterious effects on human and ecosystem health that could result from industrial geographic redistribution of Te and concentration in populated areas. Therefore, we studied Te mineralogy in ore samples in an effort to understand controls on Te accumulation in the hypogene environment. Further, we examined the behavior of Te during Au and Cu extraction processes to assess the potential for improving or initiating Te recovery from these processes economically without compromising the recovery of the primary element of interest. We also examined the surficial geochemistry of Te in historic mine tailings to assess the mineral weathering trajectory of Te in a semi-arid

climate as a model for future behavior if industrial wastes. These represent a holistic life-cycle approach to Te geochemistry from accumulation during ore formation to improper waste disposal.

3. Site Descriptions

3.1 American Smelting and Refining Company (ASARCO), Tucson, AZ

ASARCO LLC (Tucson, AZ) is the only U.S. producer of refined Te [5]. The operation is based on several mines in southern Arizona and Utah where ore is extracted, milled, and concentrated using froth flotation on site to produce the "concentrate," which is ~95% chalcopyrite. Three of the biggest deposits contributing Cu concentrate to the refinery are the Ray, Silver Bell, and Mission deposits, all of which are located in Arizona. Each deposit has different types of mineralization associated with it and contributes variable amounts of copper [80].

The principle mine studied here, the Mission Cu-Ag-Zn-Mo-Pb-Au-PGE deposit, 17 miles south of Tucson, is a skarn-related porphyry Cu deposit with seams and disseminations of chalcopyrite, bornite, covellite, chalcocite, and copper carbonates with lesser amounts of sphalerite, galena, and molybdenite [59, 80, 81]. The most abundant copper mineral is chalcopyrite. The mine produces 475,000 t of concentrated copper ore (28% Cu) annually, which equates to ~130,000 t of pure copper metal, and 2 million ounces of silver [81]. Ore concentration was by hydrothermal-metasomatic fluids migrating through altered porphyry, calc-silicate rocks, tactite, and hornfels. The highest copper grades occur in garnet-diopside skarn, where it averages about 0.7% Cu.

Copper concentrate from each mine as well as third party ores are shipped to the smelter located in Hayden, AZ. At the smelter, the concentrate is heated to 1200-1250 °C in a series of three furnaces in order to purify the copper [59]. The resultant anode copper undergoes electrolytic refining in Amarillo, TX. The byproduct of the electrolytic refining process (i.e., anode slime) is further processed to recover Te and other elements of economic interest [59]. Anode copper is shipped by truck to the Amarillo Refinery where copper is electrolytically refined and the Te-containing anode slimes are further processed to recover Te, Se, Au, Ag, and PGE.

3.2 Golden Sunlight mine, Whitehall, MT

Three main types of sulfide mineralization are found in the Golden Sunlight mine area, including Proterozoic stratabound sulfide mineralization (a broad area of sulfide mineralization spanning a broad swath of the Bull Mountain Group near Whitehall, MT), the Mineral Hill porphyry molybdenum system (a molybdenum system thought to have formed prior to the Mineral Hill breccia pipe although they have the same geographic center), and the Mineral Hill breccia pipe and related Au-bearing pyrite veins (containing 70% of Au at Golden Sunlight).The Golden Sunlight Au-Ag telluride deposit (~3 Moz Au) has proven and probable Au reserves of 127,000 ounces and total Au production in 2014 of 86,000 ounces [82]. Although grading ~0.05 oz/t, grades of up to 26 oz/t occur in veins near the porphyry center and in the deepest parts of the breccia pipe [83]. The gold telluride mineralization is genetically related to a Cretaceous alkalic-subalkalic suite of

11

dikes, sills, and stocks of quartz monzodiorite, latite to rhyolite porphyry, which intrude Proterozoic sedimentary rocks. Gold occurs as disseminations, and as structurally controlled NE and ENE trending veins and breccias along faults and joints primarily along the margins of the Mineral Hill breccia pipe. The disseminations occur in the sulfide-bearing matrix of the breccia, the latite porphyry, and the Proterozoic sedimentary rocks of the Belt Supergroup. Tellurium occurs in a variety of minerals including calaverite ($AuTe_2$), krennerite (($Au,Ag)Te_2$), sylvanite (($Au,Ag)_2Te_4$), empressite ($AgTe$), petzite (Ag_3AuTe_2), hessite (Ag_2Te), altaite ($PbTe$), native Te, coloradoite ($HgTe$), melonite ($NiTe$), tellurobismuthite (Bi_2Te_3), tetradymite (Bi_2Te_2S), buckhornite ($AuPb_2BiTe_2S_3$) and x-phase, which, according to Cabri (1965), has a composition intermediate between petzite and hessite [83]. The amount of Te as submicroscopic inclusions in pyrite is unknown. Au recovery has fluctuated (65%-85%) depending on mineralogy of ore entering the mill [49]. In large part, this variability of the output of the mine is due to large concentrations (up to 20% pyrite by mass) of pyrite-hosted Au inclusions or invisible Au in the ore body, which account for 3-25% and 6-7% of the Au, respectively [83]. Ore dressing studies indicate that optimal economic Au recovery is achieved with 37 μm particles [41, 49].

3.3 Delamar district, Lincoln County, NV

Surficial geochemistry of Te is part of an on-going study of the historic Delamar mining district in semi-arid Lincoln County, NV (**Fig. 2A**). The district operated from 1892-1938, extracting Au from quartzite host rocks with sulfide veins, and leaving 450,000 tons of tailings at the site [21]. This site contains high concentrations of Te (up to 260 mg kg^{-1}), and is popular for off road recreational travel and location near (*ca.* 25 mi) the Pahranagat National Wildlife Refuge, part of the pacific migration flyway (**Fig. 2B**).

4. Materials and Methods

4.1 Sampling

4.1.1 ASARCO: Samples were collected in March 2012 from each portion of the ASARCO copper extraction processing from the Mission mine including: hand samples of each type of ore being mined, drill core samples, and mill heads, tails, and concentrate from the north and south mills. Samples from each step in the process at the ASARCO smelter in Hayden were also obtained, as well as several samples from the Amarillo Refinery. Most samples were ground and dried prior to receipt and were stored in plastic bottles at room temperature prior to analysis.

4.1.2 Golden Sunlight: Samples of Te-bearing ore and from throughout the extraction process were collected during a June 2012 site visit. Upon receipt from Golden Sunlight mine, the samples were immediately frozen and isolated from oxygen under these conditions prior to freeze drying and analysis.

Figure 2: Historic tailings at Delamar, NV.
A) Study site located in southern Nevada; B) Regional context showing tailings transport to playa and nearby riparian corridor; C) Two tailings piles at the site with sampling locations designated stars; D) Tailings depth profile. Images: Google maps, Photos: S.Hayes.

4.1.3 Delamar: More than 100 samples were collected from the site, including: i) cores and grab samples as a function of depth from each tailings pile (**Fig. 2C, D**), ii) surficial grab samples from the 22.5 km seasonal creek leading from the tailings piles to a nearby
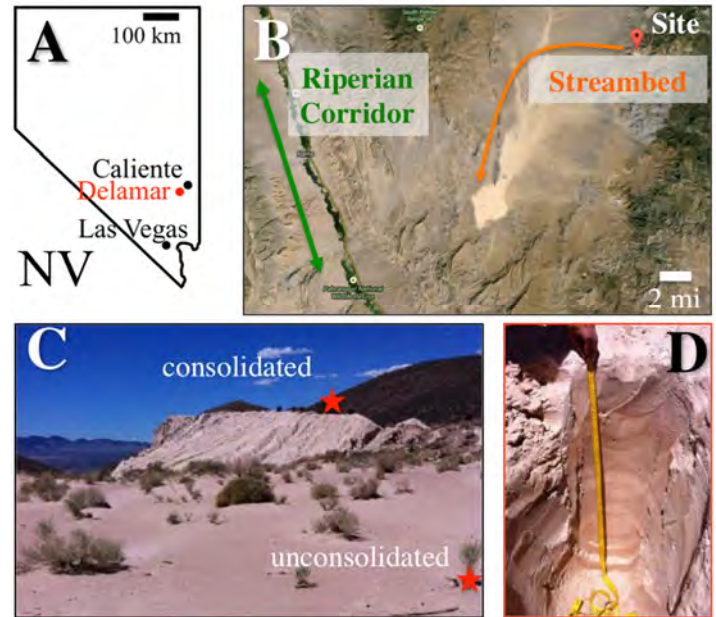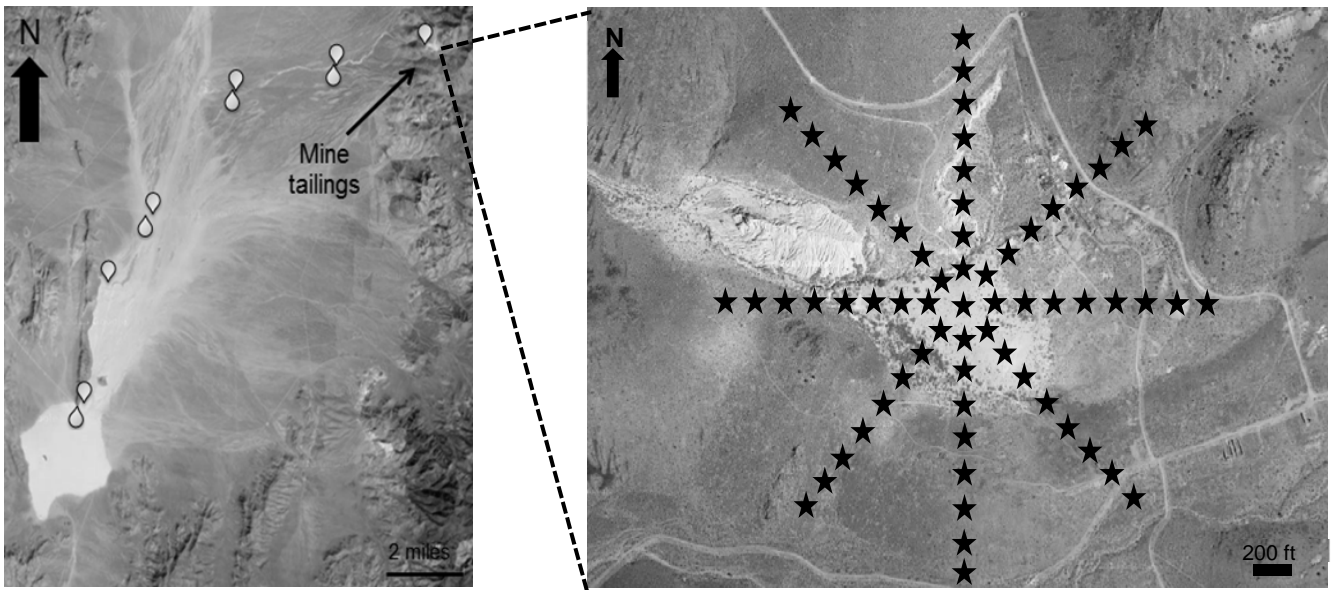

Figure 3: Location of samples collected to assess fluvial and aeolian transport.

playa (**Fig. 3**), iii) surface (0-2 cm) tailings at 150 ft intervals along eight transects radiating (N, NE, E, SE, S, SW, W, NW directions) from the center of the unconsolidated tailings and extending 1200 ft (8 samples) to assess aeolian transport of tailings near the site (**Fig. 3**), and iv) surficial control samples from ~1.8km NW of the tailings site. Upon collection, all samples were immediately frozen and isolated from atmospheric oxygen to preserve field conditions prior to transport and storage.

4.2 Physicochemical analysis

4.2.1 Elemental composition

Bulk elemental compositions were analyzed using peroxide sinter coupled with inductively coupled plasma-mass spectrometry (ICP-MS) and wavelength dispersive-x-ray fluorescence (WD-XRF). Prior to analysis, solid ICP-MS samples were dissolved using a peroxide sinter method modified after [84]. Briefly, 100 mg of sample and 600 mg of ground Na_2O_2 were mixed in a glassy carbon crucible prior to heating to 480 °C for 30 minutes. After cooling, the clinker and crucible were reacted with 10g 18mΩ water. On the analysis day, 2g of 13% HNO_3 and 2 g of 35% HCl were added to the crucible prior to dilution to a final volume of 100 mL with 18 MΩ water. Standard addition method was employed for sulfide-rich samples to ensure precise and accurate quantification using an Agilent 7500ce ICP-MS (Agilent Technologies, Santa Clara, CA). Replicate measurements of standard reference materials of hard rock mine waste (NIST-2780) and copper concentrate (CCU-1d) indicate acceptable percent differences from certified values of 8% and 6%, respectively.

Wavelength dispersive-X-ray fluorescence was used to quantify Te in higher concentration samples as well as to perform quality control checks for some ICP-MS samples. Sulfide minerals in high-grade hand samples of ore were cut to isolate pyrite or chalcopyrite in order to quantify the amount of Te in these minerals prior to grinding. Samples were micronized using ethanol in an 8000D Dual Mixer/Mill (SPEX SamplePrep; Metuchen, NJ). A minimum of 7g of grounds sample was pressed into a pellet using 20,000 psi for 2 minutes with a polyvinyl alcohol binder. After air drying, pellets were analyzed using an Axios WD-XRF (PanAlytical; Westborough, MA) equipped with an LiF 220 crystal, scintillation detector, and a 150 um collimator housed in AIL at UAF. Operating conditions were 60 kV and 66 mA with counting times of >60 s. The elements Sb, As, Bi, Co, Cu, Au, Pb, Hg, Mo, Ni, Se, Ag, S, Te, W, and Zn, along with Al_2O_3, CaO, K_2O, MgO, Na_2O, SiO_2, MnO, TiO_2, P_2O_5, and Fe_2O_3 were measured with detection limits typically on the order of a few mg kg^{-1}.

4.2.2 Bulk mineralogy

Bulk mineralogy was examined using X-ray diffraction (XRD) on 25 mm bulk powder mounts at the USGS by George Breit. Samples were hand ground to about -200 mesh prior to analysis using a Siemens D500 (Siemens, Munich, Germany) equipped with a graphite monochomator. Data were from 4 to 70 degrees two theta using Cu K-alpha

radiation using a 0.02 degree step and a count time of 1 second per step. Identification of mineral phases and the rough estimation of abundance was performed using Jade (Materials Data Incorporated, v.7) and the Powder Diffraction File.

4.2.3 Aqueous extractions

Samples were characterized using a variety of aqueous extractions performed on these tailings: (i) Saturated paste extraction (1:1 solid to solution ratio by mass, 24 hrs) followed pH measurement and elemental analysis by ICP-MS; and (ii) Physiologically-based extraction tests (PBETs) were used to determine the bioaccessible fraction of Te available for absorption after exposure by either ingestion or inhalation routes [after [76]. Extractions simulate conditions found inside alveolar macrophages and encountered in the stomach to model lung and GI tract conditions. The supernatant recovered from all extractions will be filtered and acidified prior to analysis by ICP-MS.

4.2.4 X-ray absorption spectroscopy (XAS)

The unique element specific capabilities of XAS is required to examine the atomic-scale bonding environment in samples with concentrations of ~100 mg Te kg^{-1} at the K-edge for bulk samples. Sulfur near-edge X-ray absorption fine structure (NEXAFS, referred to here as XAS) is an excellent tool to determine the S oxidation state since the white lines of S^{-II} and S^{VI} are separated by ~12 eV with detection limits down to ~2% in simple sulfide-sulfate mixtures [85]. Experiments were performed by monitoring the absorption coefficient of samples while irradiating it with tunable energy X-rays surrounding the absorption edge energy generated at Stanford Synchrotron Radiation Light source (SSRL; Menlo Park, CA). Tellurium K-edge XAS (E^0=31814 eV for TeO$_2$) were collected on beam lines 4-1 and 11-2 and sulfur K-edge XAS (E^0= 2474.02 for sodium thiosulfate) were collected on beam line 4-3. Data were reduced and analyzed using linear combination fitting in Sixpack (version 1.57; [86]) as has been described previously [85].

4.3 Grain-scale examination

4.3.1 Thin section preparation for grain-scale analyses

Prior to sectioning, unconsolidated samples (blast holes, mill samples, and mine tailings) were embedded under vacuum in EPOTEK 301-2FL epoxy and cured for three days. Several 30 μm-thick double polished thin sections were prepared for each ore sample by conventional methods (Vancouver Petrographics, British Columbia, Canada). Selected mill samples were prepared for synchrotron analysis, which required special thin section preparation using fused silica slides (Spectrum Petrographics, Vancouver, WA).

4.3.2 Electron microscopy

Electron microprobe analysis (EMPA) was performed using a JEOL JXA-8530F HyperProbe Electron Probe Microanalyzer (JEOL, Peabody, MA) at the Advanced Instrumentation Laboratory at the University of Alaska-Fairbanks (UAF) after carbon

coating using an Edwards Carbon Coating System to ensure electrical conductivity. The instrument was equipped with five WDS detectors and a Thermo System 7 silicon drift detector. Measurements were conducted using a range of accelerating voltage (15-25 kV), beam current (10-100nA), counting times (5-60 sec), magnification (45-2200x), and working distances of 10-11 cm. Sophisticated "feature sizing" software was used to locate Te-rich grains for additional analysis.

4.4 Mass balance calculations

The mass balance of Te during extraction processes was calculated in order to identify the points during refining where substantial amounts of Te were lost. The mass balance was calculated using concentrations determined using peroxide sinter ICP-MS concentrations and the flux numbers reported by ASARCO for April 2012 at the North Mission mill, March 2010 at the Hayden Smelter, and June 2012 at the Golden Sunlight mine and mill. Mass balance calculations for ASARCO were modeled after an internal bismuth mass balance study performed and supplied by ASARCO. The amount of Te conserved at each extraction point was determined by multiplying the concentration of Te ($mg \cdot kg^{-1}$) and the material flux (kg per hour or day) to determine the amount of Te (mg) and normalized to 100, according to the equation:

$$percent\ Te\ conserved = \frac{mg\ Te}{kg\ material} x \frac{kg\ material}{month} x 100\%$$

5. Results and Discussion

The distribution of Te between host minerals in ore and throughout the extraction process directly controls the behavior of Te during ore formation and during extraction processes, thus assessing the "mineral balance" is an essential first step to optimizing Te recovery, thereby optimizing future Te resources.

5.1 Tellurium behavior during Cu extraction

5.1.1 ASARCO: Te mineralogy in Cu ore

The bulk concentration of Te in copper concentrates of the mill samples varied substantially (5-15 mg Te kg^{-1}). These Te concentrations cannot be accounted for by the principle minerals found in the ore, chalcopyrite and pyrite, which have bulk Te concentrations of 7$\pm$4 (n=3) and 10$\pm$3 mg Te kg^{-1} (n=2), respectively. While these results are not conclusive, they are inconsistent with previous observations that Te is more commonly associated with chalcopyrite than pyrite [56]. Additional examination of minor elements indicates high concentrations of Te are also associated with high concentrations of other minor elements, such as Mo, Pb, and Zn. These results indicate

16

that molybdenite, galena, or sphalerite may also host high concentrations of Te. In either case, concentrations of sulfide-associated Te are too low to account for the concentrations observed in the mill concentrates, indicating the presence of a highly concentrated Te-bearing minor or trace phase. This is consistent with the telluride phases found upon examination of ASARCO Cu concentrates using EMPA (**Fig. 4**). The detection limit on EMPA analysis ($\sim$100 mg kg^{-1}) is not low enough to quantify Te substituted into sulfide minerals.
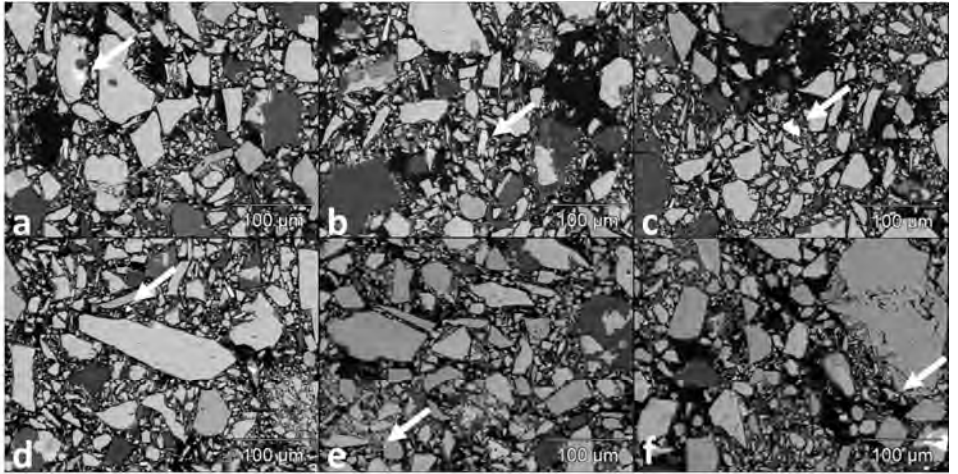

Figure 4: EMPA backscattered electron images of Cu concentrate. A) Altaite (PbTe) included in a chalcopyrite grain from the Ray Mine. B) A grain of cervelleite (Ag$_4$TeS) included in chalcopyrite from the Ray Mine. C) A grain of hessite (Ag$_2$Te) from the Ray Mine. D) A grain of tsumoite (BiTe) found in the Ray Mine concentrate. E) A grain of tsumoite found in the Mission Mine concentrate. F) A grain of pilsenite (Bi$_4$Te$_3$) from the Mission Mine complex.

The amount of Te in different ore types being mined at the Mission mine was examined by comparing the amount of Te present in blast holes sampled in April 2012. The "garnet skarn" ore contained 12 ± 2 mg Te kg^{-1}, substantially higher than any other ore types (ranging from 4.6 ± 0.9 to 0.81 ± 0.07 mg Te kg^{-1}). The mineralogy indicates that Te may not be associated with sulfides in some ore types, as sulfide minerals are not enriched, but some copper containing mineral must be present, since this ore type also contains the highest average Cu grade of any of the ore types at Mission mine [80]. Additional micro-focused analysis using electron microscopy and LA-ICP-MS was necessary to quantify the concentration and examine the distribution of Te in the suspected minor phases.

Table 3: Quantitative phase identification of Mission mine ore samples	
Blasthole description	Mineralogy
Garnet skarn (345)	50% garnet, 20% quartz, trace sphalerite, 5% calcite, and 15% other
argillite blast hole (342)	40% quartz, 30% K-feldspar, 5% calcite, 15% smectite, 10% illite or mica, trace chalcopyrite, 5% pyrite,
diopside blasthole (343)	10% calcite, 50% pyroxene, 10% garnet, 5% pyrite, trace smectite, 20% quartz, and 5% other.

5.1.2 Mass balance of Te during Cu extraction

The first critical step in determining the potential for Te recovery improvements is examining the mass balance of Te during the current extraction processes. This can be used to identify inefficient steps that might be modified to recover additional Te or extraction steps where Te accumulates that might be further processed to recover Te.

Our preliminary mass balance calculations conducted in collaboration with ASARCO indicate that only ~2% of Te present in ore is recovered for industrial use, while roughly 90% is lost during the initial milling and concentration step, which is similar to that deduced in previous studies (**Fig. 5**). This observation is somewhat perplexing because the suspected host sulfides (pyrite, chalcopyrite, molybdenite, galena, sphalerite) and gold tellurides are expected to float under the conditions used to concentrate copper [59]. Both isolated Te-bearing grains and telluride inclusions in sulfides were observed in the concentrate (**Fig. 4**). The total amount of Te in the concentrate is quite variable (5-35 mg Te kg^{-1}), likely due to variability in the Te content of different ore types, which ranges from <1 to 12 mg Te kg^{-1} in representative hand samples of different ore types from the Mission mine.

Simplified Schematic of Copper Extraction

Figure 5: Simplified Schematic of Copper Extraction. Preliminary Te mass balance calculations in parenthesis.

5.1.2.1 Smelting: Based on the volatility of other group 16 elements, particularly sulfur, and other metalloids (As and Sb), Te was expected to partition preferentially into the vapor phase [59]. Volatilized metals recondense upon cooling, forming tiny particles and may be effectively removed at the dust cleaning stage [87]. The first furnace, where SiO_2 and oxygen gas are added to oxidize sulfide minerals and trap the Fe in fayalite (Fe_2SiO_4) slag, Te concentrations are low in the slag, but highly enriched in the dust (158 ± 6 mg Te kg^{-1}). However, the flash furnace dust represents a small mass fraction of Te in the overall system. Dust from the oxidizing converter furnace and the reducing anode furnace is not substantially enriched in Te (30 ± 2 mg kg^{-1}) relative to the concentrate, but contains about half of the Te entering the smelter. Volatilized metals removed at the dust cleaning stage represent a high concentration waste stream that could be further processed to recover Te.
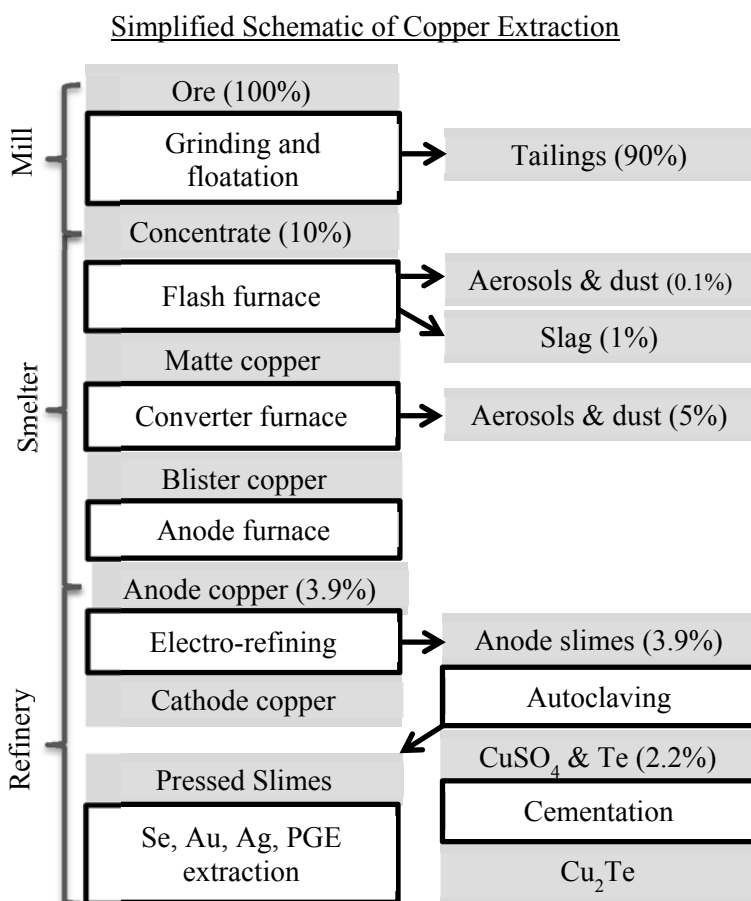
5.1.2.2 Electrorefining: The anode slimes, the waste product remaining after electrorefining of copper, contains essentially all of the Te from the copper anodes. Tellurium occurs at concentrations up to 4% by mass in the slimes as tellurides Ag(Se, Te), Cu(Se, Te), or Cu_3(Se, Te)$_2$ [59, 60]. Chen and Dutrizac performed an extensive study of tellurium behavior during electrorefining of copper [61-64]. Three forms of Te occur in copper anodes:
1. In solid solution with copper (3-10% of Te);
2. Incorporated into oxide phases with Cu, Pb, A, Sb, and Bi (~4% of Te);
3. Telluride minerals, the most common of which is Cu_2(Se,Te).

Virtually all the Te in the copper anode reports to the anode slime with less than 0.1 mg Te kg^{-1} present in cathode copper resulting from entrapment of anode slime particulates [63]. During the electrorefining process, some telluride particles react with dissolved silver and oxygen to form Ag(Se, Te), Cu(Se, Te), or Cu_3(Se, Te)$_2$. Tellurium in solid solution with copper or associated with oxide phases is released when parent phases dissolve. This liberated tellurium can become associated as tellurite (Te^{4+}) with a variety of phases, including substitution into CuO_2 as $Cu_{2-4x}Te_xO$, Cu_2TeO_3, (Cu, Ag, Pb) $TeO_3 \cdot nH_2O$ or a complex oxide phase containing Cu, Pb, Ag, Au sulfate, arsenate, antimonite, selenite, tellurite. A tellurate (Te^{6+}), $PbTeO_4$ was also reported.

Our data also reveal the presence of both oxidized and reduced Te in the raw anode slimes. XAS reveals about 1/3 oxidized Te in the raw anode slimes, likely associated with the oxidate phase described by Chen (**Fig 4**).

The anode slimes, the waste product remaining after electrorefining of copper, contains essentially all of the Te from the copper anodes and literature values report Te concentrations of up to 4% by mass [59, 60], which is similar to our value of 2.4(1)% Te by mass. Tellurium occurs in the slimes as tellurides Ag(Se, Te), Cu(Se, Te), or Cu_3(Se, Te)$_2$, and oxidized tellurite (Te^{4+}) in association with a variety of phases, including Cu_2TeO_3, (Cu, Ag, Pb) $TeO_3 \cdot nH_2O$, or a complex oxide phase containing Cu, Pb, Ag, Au sulfate, arsenate, antimonite, selenite and tellurite [62]. $PbTeO_4$ was also identified. Preliminary X-ray absorption spectroscopy fits suggest that about 1/3 of Te is oxidized in the raw anode slimes and that this proportion is not altered by the high pressure and temperature acid leach used to extract Cu and Te (**Fig. 5**). Although this leaching process is reported to be 50-80% efficient [88], the concentration of Te remains very high (2.7± 0.01% Te by mass) in the
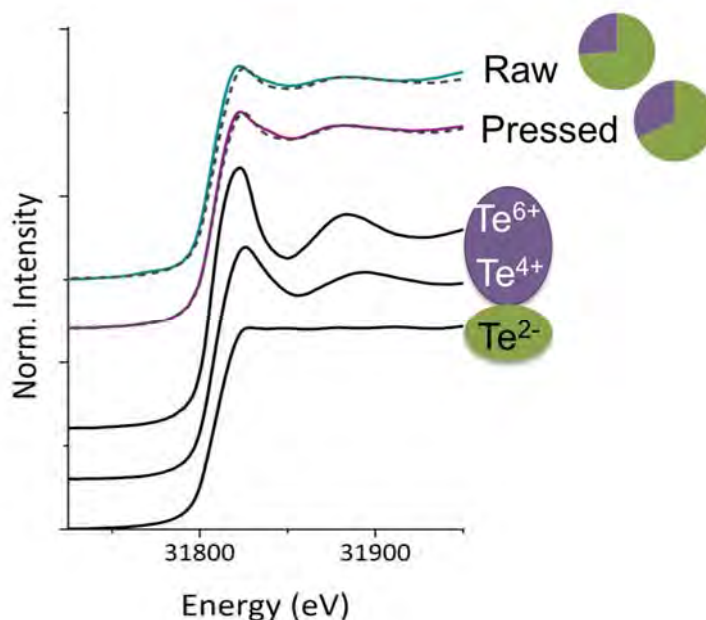

Figure 6: Tellurium speciation in ASARCO raw and pressed slimes by X-ray absorption spectroscopy (XAS).

pressed slimes, and might be further processed to recover Te prior to additional smelting for precious metal recovery.

5.1.2.3 Autoclaving: The raw anode slimes are then subjected to a high pressure and temperature acid leach to extract Cu and Te, a process reported to be 50-80% efficient [88]. However, the concentration of Te remains very high after the extraction, and might be further processed to recover Te prior to additional smelting for precious metal recovery.

At ASARCO, roughly ~60% of Te is recovered by autoclave extraction and, while bulk chemistry indicate a substantial reduction in the mass fraction of copper (28 to 6%), the concentration of Te actually increases from 2.4 to 12.7% Te by mass indicating that pressed anode slimes still contain a substantial amount of Te that might be extracted with slight tweaking of the process. Tellurium X-ray absorption spectroscopy (**Fig. 6**), indicates that Te in both the raw and pressed anode slimes is principally telluride (Te^{2-}), with a minor (~30%) amount of oxidized Te (Te^{4+} or Te^{6+}).

Overall, preliminary results indicate that only 2% of Te in ore is extracted, which leaves substantial room for improvements to Te recovery from the Cu extraction process. This preliminary work has identified several key steps in which substantial Te is either lost or accumulates that will be examined in the future in more detail. These specifically include examining the flotation behavior of Te-bearing minerals during flotation, Te speciation in smelter dusts, and optimization of autoclaving conditions to recover additional Te. Even small improvements to current rates of Te recovery would substantially increase the amount of Te available as a feedstock for industrial applications in high technology and renewable energy.

5.2 Tellurium behavior during Au extraction

Although Te is currently only produced as a byproduct of Cu mining, most Te is actually associated with alkaline igneous rocks, such as those found in the Colorado Mineral Belt, central Montana alkalic belt, and elsewhere in the western United States. Tellurium in these deposits occurs principally as tellurides, but native Te and substitution into sulfides has also been reported [48]. Gold recovery is frequently dependent on Te mineralogy because Te is one of the few elements that form minerals with Au as a principle component. Telluride mineral response to cyanide leach is highly variable and can sometimes control Au liberation during extraction, since cyanide leach is the primary technique used by modern mines to liberate gold. Tellurium-bearing ores often require pretreatment by chlorination or roasting prior to Au liberation by cyanide leach [12].

Mineralogical studies of the Golden Sunlight deposit have identified forty five minerals in four periods of hypogene mineralization [41, 83, 89, 90]. Tellurium-bearing minerals include calaverite, sylvanite, krennerite, tetradymite, tellurobismuthite, empressite, native Te, coloradoite, melonite, buckhornite, petzite and hessite. Determining the distribution of Te between telluride and sulfide minerals in ore and throughout the extraction process is an essential first step to designing a strategy for optimizing Te recovery thereby future Te resources.

5.2.1 Golden Sunlight: Te behavior during Au extraction

Although both pyrite and tellurides tend to be refractory to the cyanide leach process most commonly used in gold extraction, conditions required for the dissolution of tellurides and sulfides vary, making identifying Te host minerals key to maximizing the recovery of Te and Au [6, 7]. The response of telluride minerals to cyanide leach, the most common method of Au recovery, is generally poor and not well understood, although recovery depends on mineralogy, grinding, pH, and fO_2 [12]. Gold and silver tellurides have received the most research attention because they are known to inhibit liberation of precious metals by cyanide leach. Telluride liberation requires a higher pH (>12) cyanide leach and high dissolved O_2 content. Arsenian pyrite has also been identified as a mineral that can accumulate high concentrations of Au and Te [48].

When solubilized, Te does not form strong interactions with cyanide and the presence of both tellurite (Te^{4+}) and tellurate (Te^{6+}) species have been reported under cyanide leach conditions, depending on extraction conditions [12, 91]. The presence of Pb^{2+} and other ions to solution also inhibits surface passivation by promoting the formation of aqueous $Te(OH)_6$ rather than the precipitation of surface passifying $TeO_{2 (s)}$. Precipitation of secondary tellurite Ca and Mg salts were also reported in experiments examining telluride dissolution [92, 93]. Deschenes et al. examined the kinetics of Au liberation during cyanide leach from gold-silver telluride minerals as a function of lime addition, oxygen fugacity, lead nitrate addition, and the presence of pyrite and chalcopyrite [92]. Their results indicated the rate and extent of gold liberation from calaverite is enhanced by high pH and O_2 fugacity, directly proportional to concentration of Pb, and was reduced by the presence of sulfides. The addition of $PbNO_3$ results in the formation of a $Pb(OH)_2$ complex on calaverite surface to promote the formation of $Te(OH)_6$, which does not passify the surface and reduces the activation energy for Te oxidation and solubilization.

The calculation of a mass balance for Te in the Golden Sunlight deposit was unsuccessful, due to the heterogeneous nature of the ore coming into the mill with respect to Te content. The distribution of Te in the deposit as based on whole rock data throughout the deposit supports this contention [94]. Nonetheless, the concentrations of Te measured throughout the extraction process lend insight into the value of continued examination of Te recovery from Au mining (**Fig. 7**). However, high concentrations of Te in some stages of the process indicate Te recovery from Au extraction may be economic if additional fundamental information were available.
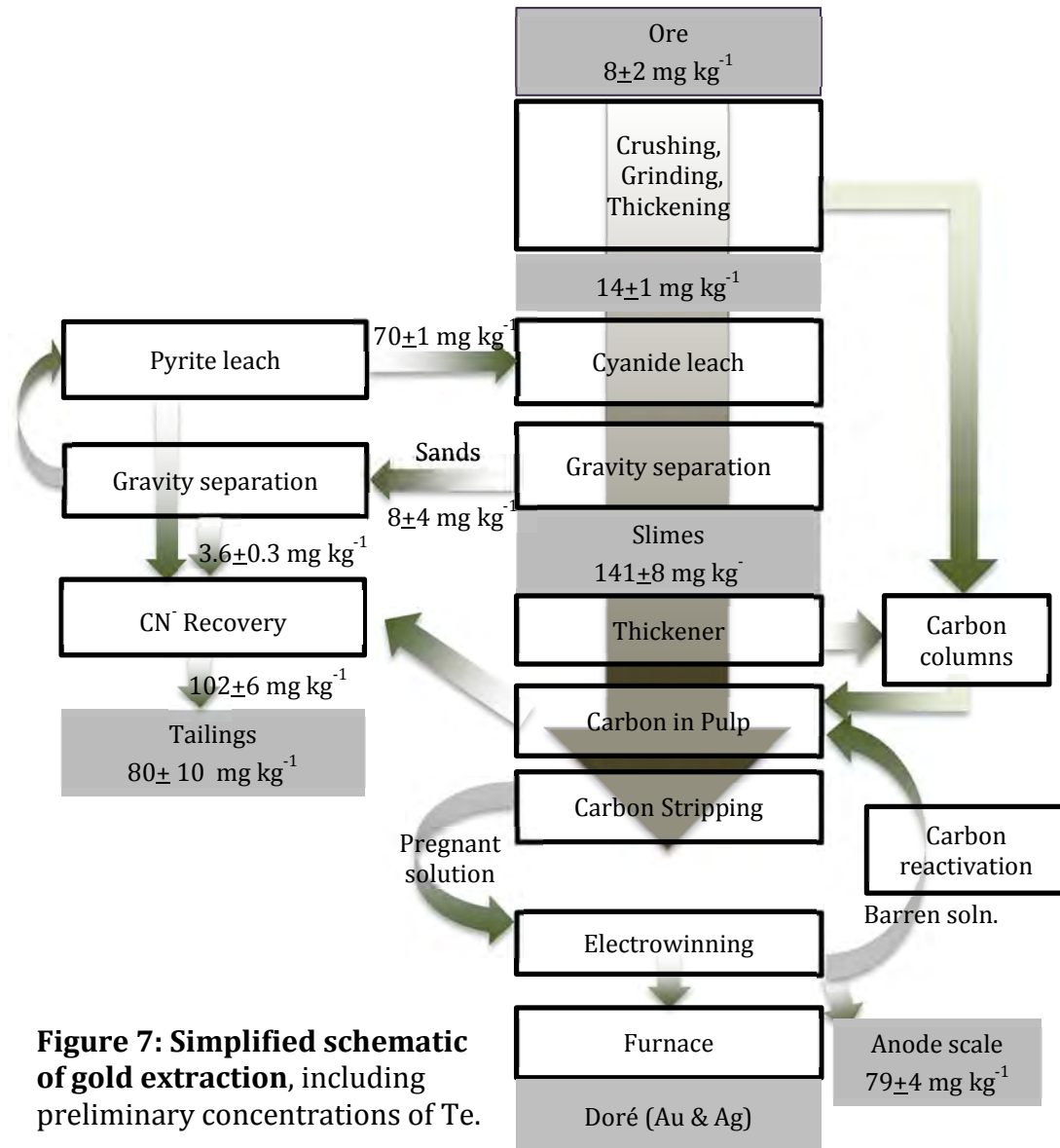
Figure 7: Simplified schematic of gold extraction, including preliminary concentrations of Te.

Process flow	Te concentration
Ore	8 ± 2 mg kg^{-1}
Crushing, Grinding, Thickening	14 ± 1 mg kg^{-1}
Pyrite leach	70 ± 1 mg kg^{-1}
Cyanide leach	
Gravity separation (Sands)	8 ± 4 mg kg^{-1}
Slimes	141 ± 8 mg kg^{-}
Gravity separation	3.6 ± 0.3 mg kg^{-1}
CN^{-} Recovery	102 ± 6 mg kg^{-1}
Thickener	
Carbon columns	
Carbon in Pulp	
Tailings	80 ± 10 mg kg^{-1}
Carbon Stripping	
Carbon reactivation	
Pregnant solution / Barren soln.	
Electrowinning	
Furnace	
Anode scale	79 ± 4 mg kg^{-1}
Doré (Au & Ag)	

5.3 Surficial Te geochemistry

Because of low abundance and limited historic industrial use, the environmental controls responsible for determining Te mobility have not garnered much research attention. However, with increasing demand and widespread use, an improved understanding of controlling factors is essential to informed policymaking. The speciation of metals in the environment is dependent on redox potential, pH, adsorption-desorption kinetics, (co)precipitation-dissolution reactions, and microbially-mediated processes. These biogeochemical reactions, which can vary widely under near-surface conditions, are expected to dramatically alter contaminant mobility and toxicity.

Figure 8: Metal(loid) concentrations as a function of depth in the Delamar mine tailings.

Bulk chemical analysis of the grab samples collected from the top 2 m of the tailings as a function of depth indicate the accumulation of Te and other toxic metal(loid)s at the tailings surface, potentially as efflores cent salts or sorbed species (**Fig. 8**). Efflorescent salts have been shown to be persistent in semi-arid environments due to the low availability of liquid water and have further been shown to be readily transportable and bioaccessible [68, 69]. Iron (oxy)hydroxides are also common minerals in mine tailings and have been shown to control the sequestration and release of metal(loid)s of concern in semi-arid tailings [69, 85, 95]. Previous studies have noted a strong affinity of Te oxyanions for iron (oxy)hydroxides in marine and surficial environments [15, 77, 96], making association with iron (oxy)hydroxides a likely sink of Te in oxyanions in the surficial environment.

Studies of the surficial tailings using electron microscopy reveals two distinct populations of Te are present at the surface of the tailings (**Fig. 9**). The
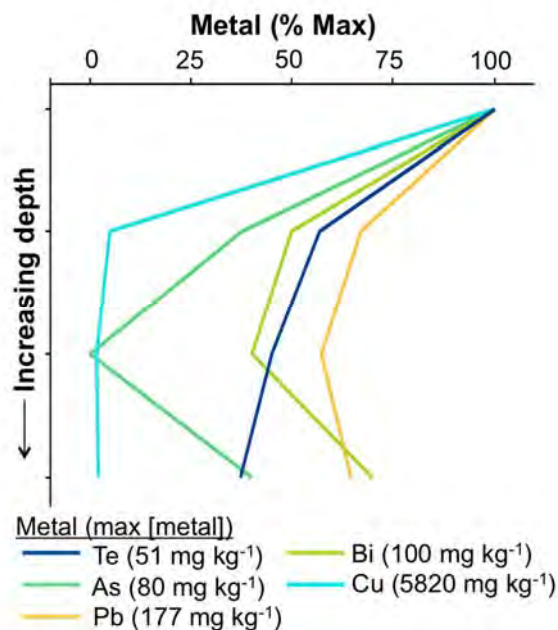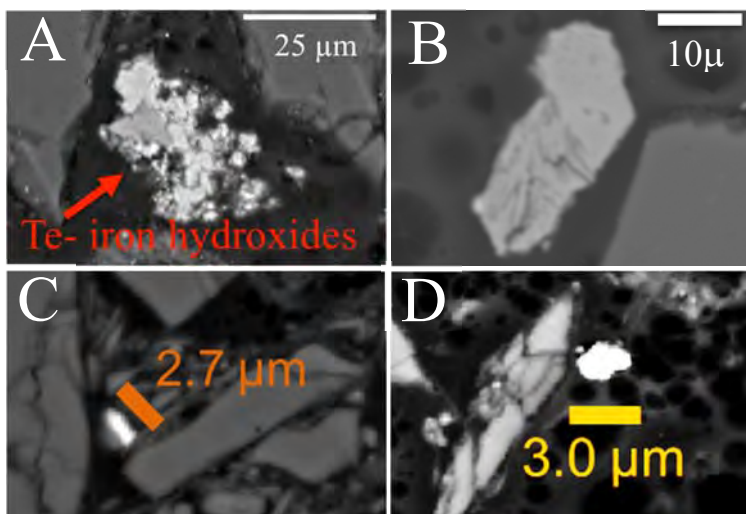

Figure 9: Electron microscopy of Te-containing particles. A) Tellurium association with iron (oxy)hydroxides, B) Te-rich particle with low iron (Table 4, particle 11), C &D) tiny Te-bearing particles.

23

majority of the particles located containing Te were identified as iron oxides, most likely goethite (α-FeO(OH), 62.9% Fe by mass), hematite (Fe_2O_3, 69.9% Fe by mass), or ferrihydrite (FeO(OH), 62.9% Fe by mass) due to the observed 48.4-67.2% Fe by mass (**Table 4**). However, a few Te-containing particles contain a larger mass fraction of Te (**Table 4**, particle 11). Tellurium can also occur in very small (<5 μm) particles, which are likely to be transportable by wind, readily inhaled deeply into lungs (**Fig. 9 C, D**).

Tellurium speciation was examined using XAS and indicates that Te exists principally as tellurate in surficial tailings (**Fig 10**). Physiologically based extraction tests indicate that bioaccessibility in simulated lung is low (less than 1% of Te solubilized), which is critical because inhalation is the most likely human exposure during recreational activities like operating off-road vehicles. In simulated gastrointestinal fluid, more Te from surficial mine tailings was liberated (2- 21 % of Te). Together, these indicate low lung bioaccessibility and medium gastric bioaccessibility. This is consistent with tellurate as the dominant species as tellurate salts tend to be insoluble.
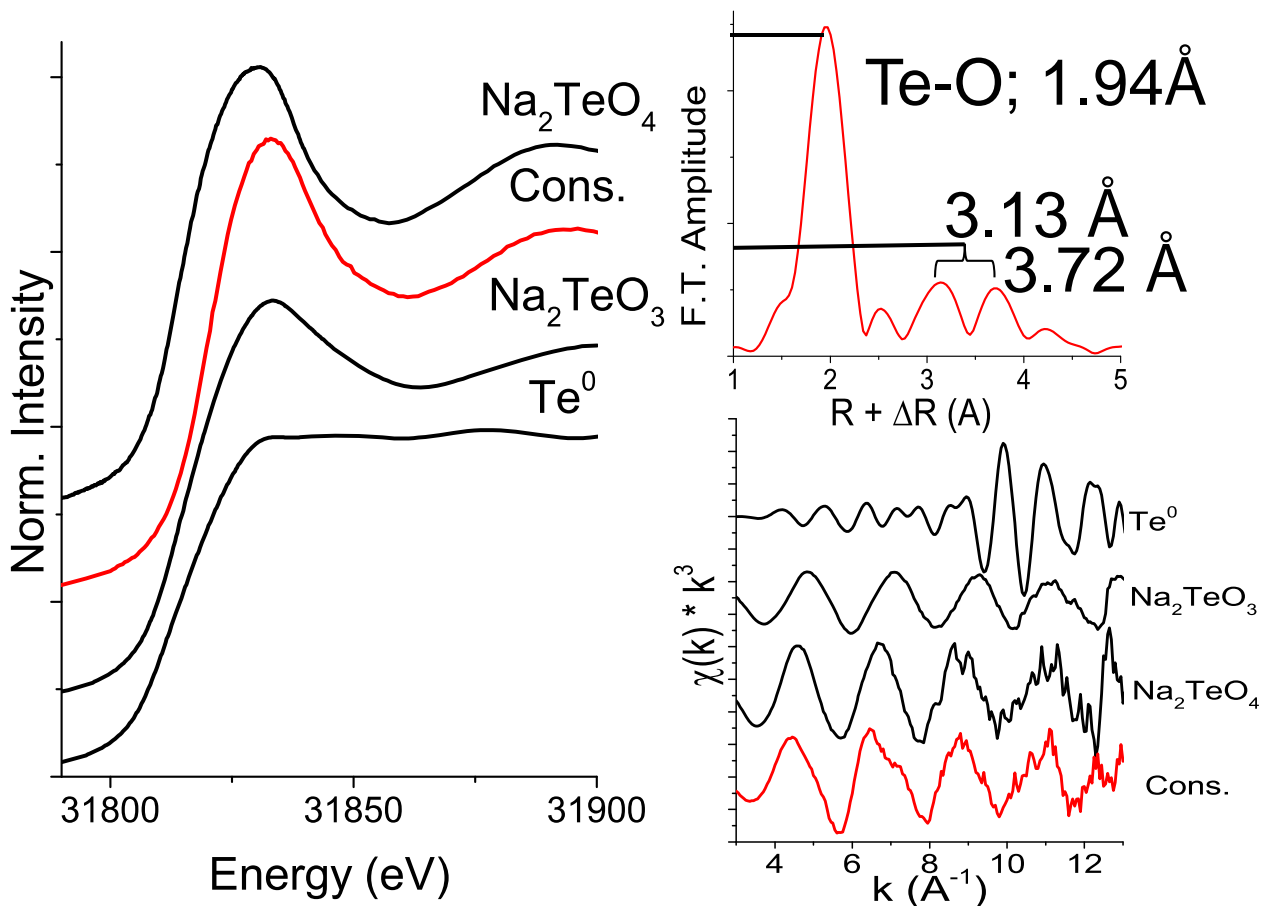

Figure 10: Tellurium speciation in surficial Delamar tailings. Tellurium is principally present as tellurate (Te^{6+}).

24

Table 4: Quantitative chemical analysis of Te-containing spots by EPMA (percent composition by mass)

Grain:	1	2	3	4	5	6	7	8	9	10	11	12
O:	24.1	32.2	24.6	20.8	28.8	34.3	27.6	26.3	28.4	26	21	26.6
Fe:	63.2	48.4	66.7	66.7	60.2	2.3	62.5	67.2	60.5	61.3	2.7	61.7
Te:	1.8	2.4	3.5	1.9	2.3	0.6	2.5	0.7	4.5	4.7	30.9	1.7
F:	0	0.8	0	0	0	0	0	0	0	0	0	0
Na:	0.8	0.9	0	0	0.5	0.1	0.5	0.6	0.5	1.3	0.6	1.8
Mg:	0	0.3	0	0	0.2	0	0	0.2	0.1	0.1	0.1	1.2
Al:	0.3	2.1	0.2	2.4	1.7	0.2	0.3	0.3	0.9	0.2	0.6	1.3
Si:	1.4	5.5	1.1	3.5	1.6	0.4	1.9	1.9	1.5	1.5	4.4	3.5
P:	0.2	0.2	0.2	0.1	0.5	0	0.2	0.1	0.3	0.5	0	0.1
S:	0	0.1	0.2	0.2	0.3	0	0	0.2	0.5	0.3	0	0.4
Cl:	0	0.2	0.1	0.1	0	0	0.2	0.1	0.2	0.3	0	0.2
K:	0	0.8	0	0	0.2	0	0.1	0.3	0.2	0.2	0.1	0.3
Ca:	0.4	0.4	0.4	0.3	0.6	0.1	0.5	0.3	0.5	0.3	7.3	0.3
Ti:	0	0	0	0	0.1	60.4	0.1	0	0	0	0	0
Mn:	0.1	0.1	0.1	0	0	0.1	1.8	0	0.2	0.1	10.7	0.2
Cu:	0.5	3.7	0.2	1	0.2	0	0.1	0.3	0.4	1.9	1.1	0.1
Zn:	0	0.7	0	0.2	0.1	0	0.1	0	0.1	0.2	0.2	0.1
As:	0.6	0.4	0.5	0.3	1.5	0	0.1	0.2	0.6	0.9	2.6	0.4
Mo:	0.7	0	0.2	0.3	0	0	0	0.1	0.1	0	1.6	0
Sb:	0.9	0	0.3	0.7	0.8	0.1	0.2	0.2	0.2	0.2	0.3	0
Tl:	0.4	0.1	0	0.2	0	0.7	0	0.3	0.2	0	0	0
Pb:	0	0.6	0	0	0	0.7	0.3	0.7	0	0	10.6	0
Bi:	4.6	0.1	1.7	1.1	0.1	0	0.9	0	0.2	0	5.2	0.2

5.4 Transport of Te containing particles

Google Earth images of the Delamar site (**Fig. 2 B**) show evidence of surface-water transportation of tailings down gradient to a sparsely vegetated playa. Samples were collected along this dry streambed and analyzed for Te and other metal(loid)s concentrations (**Fig. 3**). The results indicate substantial metal(loid) transport downstream of the mine tailings with a decrease in concentration with distance away from the site. However, the expected logarithmic decay of metal(loid) concentrations reported at other sites [73] was confounded by the highest concentration of all elements just downstream of a road (**Fig. 11 A, B**), indicating that other activities in the area may contribute to metal(loid) dispersion. There is a history of mining in this area and ore trucks may have dispersed metal(loid)s near roads, as was reported previously [73]. Of note is that Zn concentrations increase in samples collected downstream of the confluence with the larger stream from the north, indicating the presence of another source of Zn to the environment (**Fig. 11 A**). Lead and Cu concentrations are highly correlated with Te (**Fig. 11 C**), suggesting that Cu and Pb may act as tracers for lower concentrations of Te in these streambed sediments and may also indicate sorption of these metals to iron (oxy)hydroxide phases.

Wind dispersion of metal(loid)-bearing particles is also a likely dominant transport mechanism in semi-arid environments [87]. HYSPLIT modeling (not shown) is
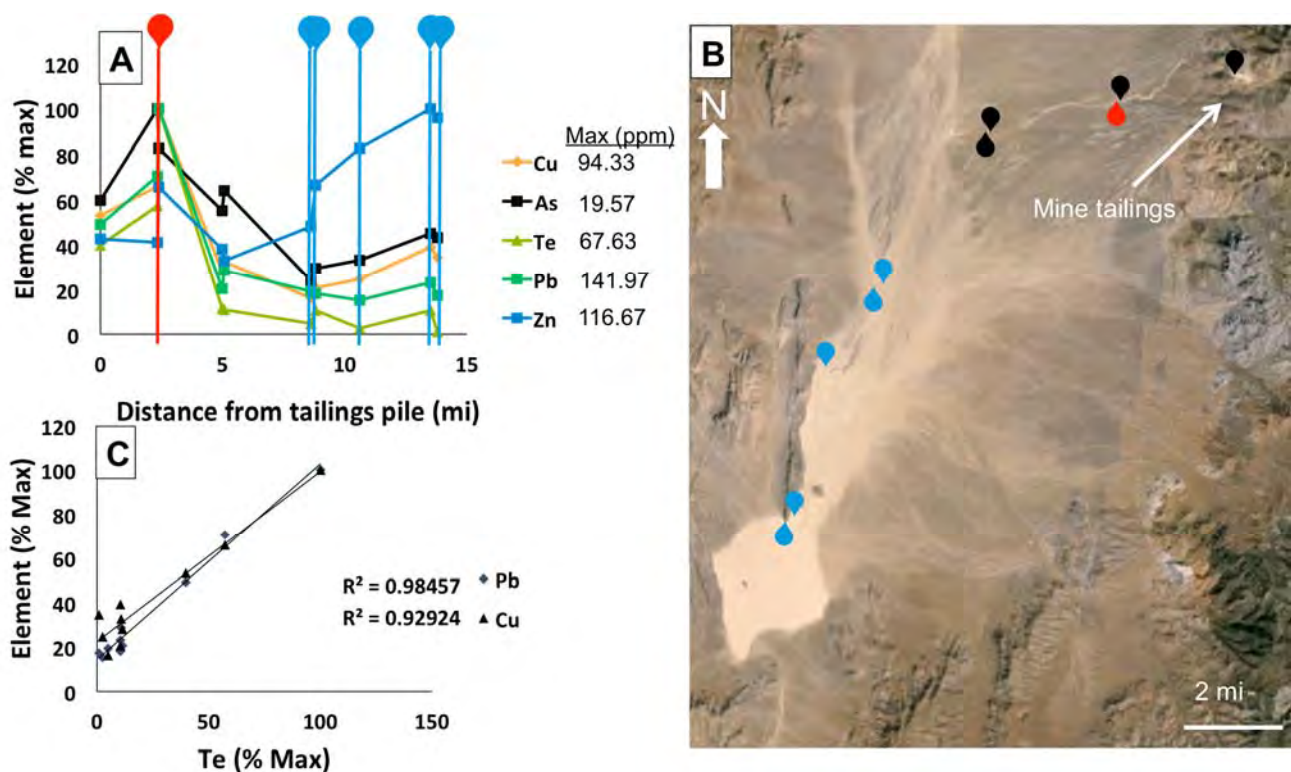

Figure 11: Surface water transport of tailings. A) concentrations of Te and other metals in the streambed sediments, B) Map of sampling locations, C) correlation between tellurium concentrations and lead and copper.

consistent with the direction of dominant southwest continental winds, and indicates the

dominant wind direction at the site is from SW to NE. However, HYSPLIT also indicates particles from the tailings piles or playa could be transported in a variety of directions, including toward the Pahranagat National Wildlife Refuge or nearby population centers, Las Vegas and Caliente. Short term anemometer data from June, 2014 sampling days indicate that down valley WNW is the dominant wind direction (**Fig. 12A**). HYSPLIT modeling for the same time period indicates winds from SW to NE (**Fig. 12B**), highlighting the complicating influence of local topography. Although the trends in wind direction are not consistent, Te concentrations in surficial samples indicate Te enrichment in surficial samples surrounding the mine tailings (**Fig. 12 C**). Some samples in the grid were collected on top of other historic tailings piles or other mining related facilities, and can thus be excluded from the analysis of aeolian transport. Tellurium concentrations are somewhat enriched toward the west, which supports the short-term anemometer data indicating down valley transport, while the distribution of other elements do not show a clear pattern (**Fig. 12 D, E**). The anticipated logarithmic decay of metal concentrations as a function of distance from the site was not observed [68, 73].

6. Conclusions and Future Directions

6.1 Potential for Te recovery from Cu and Au extraction

The goal of this study was to determine the potential for additional Te recovery from current extraction processes of Cu and Au. The mineralogy of Te in the ore is somewhat complex and will require additional study to determine the distribution of Te between sulfides and telluride minerals as well as the relative amounts of telluride minerals in each ore type. However, it is clear that there are high concentrations of Te present in some waste products of Cu and Au extraction, and additional Te might be recovered from these processes. In the case of copper, only 2% of Te in the ore is recovered for industrial use. During the initial concentration of copper ore minerals, roughly 90% of Te was lost. In the case of gold, the heterogeneous nature of the mill feed did not allow an accurate determination of mass balance, but high concentrations of Te were measured in the mill.

Improving or initiating recovery Te from operating copper and high-grade telluride deposits is one potential method of increasing near-term Te supply. Currently, ASARCO is the only domestic producer of Te, and even small improvements to recovery rates would substantial increase the amounts of industrially available Te.

In future work, we plan to examine the mineralogy and tellurium content of the mill heads, tails, and concentrate in order to assess the behavior of Te-bearing minerals. Additionally, we propose to perform flotation experiments to directly examine the behavior of Te-bearing minerals identified in ore using electron microscopy. The proposed floatation experiments will be performed at the bench scale using a mixture of Cu mine mill feeds and well-characterized high-grade Te-bearing ores with high concentrations of minerals identified from the Cu ores.
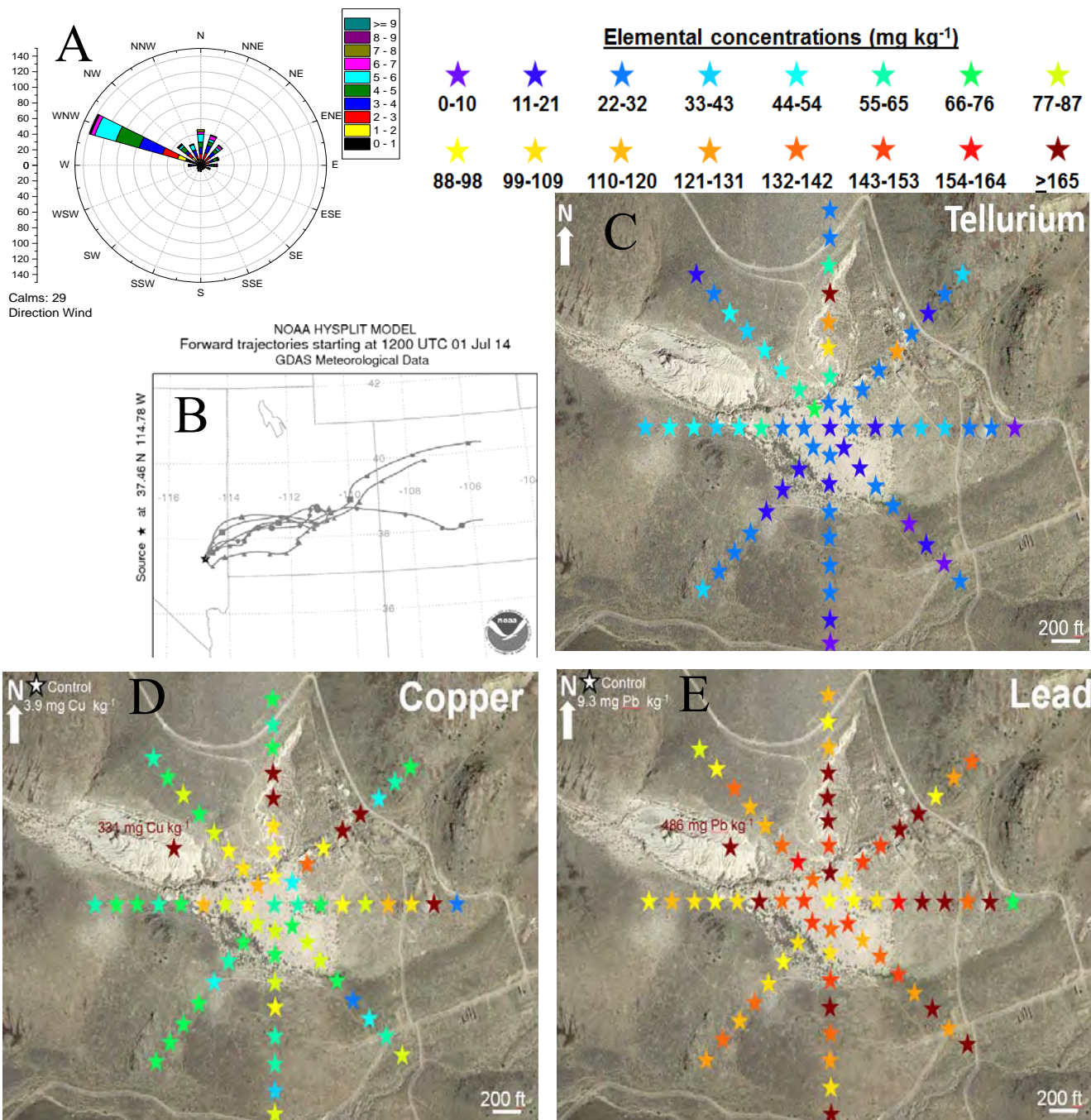
Figure 12: Aeolian transport of tailings. A) Short-term anemometer data, B) HYSPLIT modeling of winds at Delamar, NV June , 2014. C) Tellurium, D) Copper, and E) Lead concentrations as a function of distance from the center of the largest tailings pile.

6.2 Tellurium speciation in the surficial environment

Surficial Te speciation, bioaccessibility, and transport were examined at Delamar, NV to determine if tellurium released to the surficial environment poses a health threat to

nearby populations and ecosystems. Reduced Te-bearing minerals released during the mining process or from industrial activities are likely to undergo oxidative weathering to tellurium oxyanions, tellurite or tellurate, in the surficial environment. Indeed, preliminary results suggest that Te in semi-arid surficial tailings is principally the least toxic, more oxidized tellurate, and often associated with iron (oxy)hydroxides. There was also an observed accumulation of Te and other metal(loid)s of environmental concern at the surface of the tailings, sometimes in small, readily transportable particles, but that overall bioaccessibility was 2-20% Te.

Transport by both wind and surface water were observed in samples collected from the streambed and downwind of the tailings. These results indicate that after 75 years of weathering, nearly all surficial Te is present as less bioaccessible tellurate, but that the Te-bearing particles are enriched at the surface and small enough to be readily transported. Taken together, this demonstrates that Te is not as potentially harmful as it might be at the site examined in detail by this study. Future studies will extend this examination of Te speciation and bioaccessibility as a function of climate to determine if other climatic regimes might be stable for the more toxic tellurite species.

7. Acknowledgments

8. Resulting proposals, presentations, and publications involving Te geochemistry, mineralogy and geology (Graduate student author, *Undergraduate student author*)

Proposals

Hayes, S.M., and Webb, S.M. *Proposal extension: Environmental speciation and mobility of tellurium*. Stanford Synchrotron Radiation Lightsource. Active: 2012-2014

Hayes, S.M., and Spry, P.G. *Tellurium speciation in common sulfide minerals: implications for exploration and extraction*. Advanced Photon Source. June, 2013

Witte, R.L, and Hayes, S.M. *Evaluating potential for recovery of Te as a byproduct of Au extraction*. UAF URSA Research Proposal. November, 2013. Funded Spring 2014, $1,890.

Hayes, S.M., and Spry, P.G. *Optimizing Au (and potentially Te) recovery from the CC&V mill through correlating Au and Te mineralogy with element liberation during cyanide leach*. Submitted to Cripple Creek and Victor Mine (part of AngloGold Ashanti). June 2014

Hayes, S.M., and Spry, P.G. *Optimization of tellurium byproduct recovery from operating mines in support of energy technologies*. Submitted to Critical Metals Institute (Ames, IA). July 2014 (not funded).

Smith, D., and Holwell, D. *Te and Se cycling and supply (TeaSe)*. Submitted to Natural Environment Research Council, United Kingdom. July 2014. Role: Hayes and Spry are Project Partners. Funded Spring 2015, ~$4,400,000

Hayes, S.M., Spry, P.G., and Akdogan, G. *Collaborative research: Optimization of tellurium byproduct recovery from operating mines in support of energy technologies*. Submitted to NSF-CBET-CBS. November 2014 (not funded).

Milke, K., and Hayes, S.M. *Environmental health impacts of tellurium transport in mine tailings*. Funded Spring 2015 $6,000.

Knight, N.A., and Hayes, S.M. *Assessment of tellurium in semi-arid mine tailings at Delamar, Nevada: Implications for human and ecosystem health*. Funded Spring 2015, $9,000.

Abstracts of Presentations

Hayes, S.M., Foster, A.F., and Balistrieri, L. **2011**. *Study of tellurium in environmental and industrial samples*. American Chemical Society Meeting, Anaheim, CA. Talk. March 27, 2011.

Fornadel, A.P., Spry, P.G., Voudouris, P. C., and Melfos, V. **2011**. *Mineralogical, stable isotope, and fluid inclusion studies of spatially related porphyry Cu-Mo and epithermal Au-Te mineralization, Fakos Peninsula, Limnos Island, Greece*. Geological Association of Canada/Mineralogical Association of Canada, Abstracts, v. 34, p. 66.

Hayes, S.M., Foster, A.F., and Balistrieri, L. **2012.** *Study of tellurium in environmental and industrial samples*. Geological Society of America Meeting, Charlotte, NC. Poster. November 4, 2012.

Skidmore, A.E., Spry, P.G., and Hayes, S.M. **2013**. *Tellurium speciation and recovery during Cu ore processing*. Geological Society of America Meeting, Denver, CO. Talk. October 30, 2013.

Knight, N.A., and Hayes, S.M. **2013**. *Tellurium speciation and distribution as a function of depth in semi-arid mine tailings*. Geological Society of America Meeting, Denver, CO. Poster. October 29, 2013.

Hagnegahdar, M. A., Schauble, E.A., Fornadel, A.P., and Spry, P.G. **2013**. *First-principles models of equilibrium tellurium isotope fractionation*. Eos Transactions American Geophysical Union, Abstract V51A-2636.

Hayes, S.M., Skidmore, A.E., Witte, R.L., and Spry, P.G. **2014**. *Supplying tellurium for use in high technology by optimizing current mining processes*. Geological Society of America Meeting, Vancouver, BC. Poster. October 19, 2014.

Fornadel, A.P., Spry, P.G., Schauble, E., Hagnegahdar, M., Mathur, R.D., and Jackson, S.E. **2013**. *Stable Te isotope variability in ore-forming systems: Causes and magnitude*. Society of Economic Geologists Meeting (Whistler, British Columbia), Abstract Volume, Poster. p. 40.

Knight, N.A, and Hayes, S.M. **2014**. *An assessment of tellurium in semi-arid mine tailings at Delamar, NV: Implications for Human and Ecosystem Health*. Goldschmidt Meeting, Sacramento, CA. Poster. Geological Society of America Meeting, Vancouver, BC. Poster. October 20, 2014.

Hayes, S.M., Skidmore, A.E., *Witte, R.L.*, and Spry, P.G. **2014**. *Supplying tellurium for use in high technology by optimizing current mining processes*. SSRL User Meeting. Poster.   October 8, 2014.

Witte, R.L., Skidmore, A.E., Spaleta, K.J., and Hayes, S.M. **2014**. *Evaluating Potential for Recovery of Te as a Byproduct of Au Extraction*. UAF Research Day. Poster. May 28, 2014

Hayes, S.M., Skidmore, A.E., and Spry, P.G. **2014**. *Extraction of Te for use in high tech as a byproduct of current mining processes.* Goldschmidt Meeting, Sacramento, CA. Talk. June 5, 2014

Hagnegahdar, M. A., Schauble, E.A., Fornadel, A.P., and Spry, P.G. **2014**. *First-principles models of equilibrium tellurium isotope fractionation*. Goldschmidt Conference, Sacramento, CA. Poster Abstracts, p. 893. June 5, 2014.

Knight, N.A., and Hayes, S.M. **2014**. *Tellurium speciation and distribution as a function of depth in semi-arid mine tailings*. Goldschmidt Meeting, Sacramento, CA. Poster. June 5, 2014.

Knight, N.A., and Hayes, S.M. **2015**. *Assessment of tellurium in semi-arid mine tailings at Delamar, Nevada: Implications for human and ecosystem health*. American Chemical Society Meeting. Talk. March 20, 2015.

Invited Presentations

Spry, P. G. *The connection between Au and Te in hydrothermal gold telluride deposits*
Department of Mineralogy, Petrology and Economic Geology, Aristotle University of Thessaloniki, Greece (May 10, 2012)
Stockholm University, Sweden (March 23, 2012)
Montanuniversität, Leoben, Austria (March 27, 2012)
Département de Minéralogie, Université de Genève, Switzerland (March 29, 2012)
Swiss Institute of Technology – ETH, Switzerland (April 28, 2012)
Department of Mineralogy-Petrology, University of Athens, Greece (May 8, 2012)
Department of Geological Sciences, East Carolina University (September 28, 2012)
Department of Geosciences, University of Arizona (January 7, 2013)
Department of Earth and Ocean Sciences, University of British Columbia (January 25, 2013)

Spry, P. G. *The Stanos Au-Cu-Bi-Te deposit, northern Greece*
Eldorado Gold Corporation, Vancouver, British Columbia, Canada (January 25, 2013)

Hayes, S.M. *Geochemistry of tellurium: resources, extraction, and weathering*. 2013 SSRL User Meeting, Session: Synchrotron Techniques in Metal Biogeochemistry: Across Time and Spatial Scales. (October 2, 2013)

Hayes, S.M., Spry, P.G. *Tellurium Geochemistry: Surficial Weathering and Extraction.* Te and Se Research Challenges Workshop, Leicester, United Kindgom. Invited Participant. (January 12, 2014)

Hayes, S.M. *Tellurium recovery from copper mining*. UAF Department of Chemistry and Biochemistry Seminar. (March 4, 2014)

Hayes, SM; Skidmore, AE; Knight, NA; *Milke, KP*; *Knight, D*; Spry, PG. 2015. *Tellurium: Industrial supply and surficial geochemistry*. US Geological Survey, Reston office. Invited talk. (May 21, 2015)

Hayes, SM; Skidmore, AE; Knight, NA; *Milke, KP*; *Knight, D*; Spry, PG. 2015. *Tellurium: Industrial supply and surficial geochemistry*. Colorado College. Invited talk. (July 9, 2015)

Hayes, SM; Skidmore, AE; Knight, NA; *Milke, KP*; *Knight, D*; Spry, PG. 2015. *Industrial supply and surficial geochemistry of tellurium*. US Geological Survey, Denver office. Invited talk. (July 15, 2015)

Hayes, SM; Skidmore, AE; Knight, NA; *Milke, KP*; *Knight, D*; Spry, PG. 2015. *Tellurium: Industrial supply and surficial geochemistry*. Western State Colorado University. Invited talk. (July 21, 2015)

Hayes, SM. 2015. *Supplying tellurium for use in high technology by optimizing current mining processes*. Alaska Miners Association. Invited talk. (November 13, 2015)

Hayes, SM. 2015. *Industrial supply and surficial geochemistry of tellurium*. UAF WERC seminar. Invited talk. (January 16, 2016)

Manuscripts

Fornadel, A.P., Spry, P.G., Mathur, R.D., Jackson, S.E., and Chapman, J.B. **2012**. *Methods for the determination of Te isotope systematics of minerals in the system Au-Ag-Te by MC-ICP-MS*. Mineralogical Magazine, 76 (6), p. 1714.

Fornadel, A.P., Voudouris, P. C., Spry, P.G., and Melfos, V. **2012**. *Mineralogical, stable isotope, and fluid inclusion studies of spatially related porphyry Cu-Mo and epithermal Au-Te mineralization, Fakos Peninsula, Limnos Island, Greece*. Mineralogy and Petrology, v. 102, p. 85-111.

Voudouris, P., Spry, P.G, Sakellaris, G.-A., Mavrogonatos, C.G., Bristol, S., Melfos, V., and Fornadel, A.P. **2013**. *Bismuthinite derivatives, lillianite homologues and bismuth sulfotellurides as indicators for gold mineralization at the Stanos shear-zone-related prospect, Chalkidiki, northern Greece*. Canadian Mineralogist, v. 51, 119-142.

Alfieris, D., Voudouris, P., and Spry, P.G. **2013**. *High-intermediate sulfidation epithermal Pb-Zn-Cu-Au-Ag-Te mineralization at western Milos Island, Greece: Mineralogical and geological constraints on ore formation in a shallow submarine setting*. Ore Geology Reviews, v. 53, p. 159-180.

Voudouris, P., Melfos, V., Spry, P.G., Kartal, T., Schleicher, Arikas, K., Moritz, R., and Ortelli, M. **2013**. *The Pagoni Rachi-Kirki Mo-Re-Cu-Au-Ag-Te deposit, northern Greece: Mineralogical and fluid inclusion constraints on the evolution of a telescoped porphyry-epithermal system*. Canadian Mineralogist, v. 51, p. 253-284.

Grundler, P.V., Brugger, J., Etschmann, B., Helm, L., Liu, W., Spry, P.G., Tian, Y., Testemale, D., and Pring, A. **2013**. *Speciation of aqueous tellurium (IV) in hydrothermal solutions and vapors and the role of oxidized tellurium species in gold metallogenesis*. Geochemica et Cosmochimica Acta, v. 120, p. 298-325.

Bindi, L., Voudouris, P. Ch., Spry, P.G., and Menchetti, S. **2013**. *Structural role of tellurium in the minerals of the pearceite-polybasite group*. Mineralogical Magazine, v. 77, p. 419-428.

Fornadel, A.P., Spry, P.G., Mathur, R.D., Jackson. S.E., Chapman, J.B., and Girard, I. **2014**. *Methods for the determination of Te isotopes of minerals in the system Au-Ag-Te by MC-ICP-MS*. Journal of Analytical and Atomic Spectroscopy, Journal of Analytical and Atomic Spectroscopy, v. 29, p. 623-647.

Bristol, S.K., Spry, P.G., Voudouris, P., Melfos, V., Mathur, R.D., Fornadel, A.P., and Sakellaris, G.-A. **2015**. *Geochemical and geochronological constraints on the formation of shear-zone hosted Cu-Au-Bi-Te mineralization in the Stanos area, Chalkidiki, northern Greece*. Ore Geology Reviews, v. 66, p. 266-282.

Kelley, K.D., and Spry, P.G. **2016**. *Critical metals associated with alkaline-rock related epithermal gold deposits*. Reviews in Economic Geology, v. 18, p. 195-216.

Bindi, L., Stanley, C.J., and Spry, P.G., Cervelleite. **2015**. *Ag₄TeS: solution and description of the crystal structure*. Mineralogy and Petrology, v. 109, p. 413-419.

Bindi, L., Stanley, C.J., and Spry, P.G. **2015**. *New structural data reveal benleonardite as a member of the pearceite-polybasite group*. Mineralogical Magazine, v. 79, p. 1217-1227.

Fornadel, A.P., Spry, P.G., Schauble, E.A., Hagneghadar, M.A., Jackson. S.E., and Mills, S.J., Theoretical and measured stable Te isotope fractionation in tellurium-bearing minerals in precious metal hydrothermal ore deposits. Geochimica et Cosmochimica Acta, in review.

Skidmore, A.E., Spaleta, K.J., Spry, P.G., and Hayes, S.M. *Tellurium speciation and recovery during Cu ore processing*. For submission to Metallurgical Transactions B-Process Metallurgy.

Spaleta, K.J., *Witte, R.L.*, Skidmore, A.E., Spry, P.G., and Hayes, S.M. *Evaluating potential for recovery of Te as a byproduct of Au mining at the Golden Sunlight mine (Whitehall, MT)*. For submission to Geostandards and Geoanalytical Research.

Knight, N.A., and Hayes, S.M. *An assessment of tellurium in semi-arid mine tailings at Delamar, NV: Implications for Human and Ecosystem Health*. For submission to Environmental Science and Technology.

9. References

1. Jaffe, R., et al., *Energy Critical Elements: Securing Materials for Emerging Technologies*. 2011, American Physical Society: Washington, DC.
2. Price, J.G., *The world is changing*. Society of Economic Geologists Newsletter, 2010. **82**.
3. DOE, *Critical Materials Strategy*. 2011.
4. *Critical Elements for New Energy Technologies*, in *MIT Energy Initiative Workshop Report, April 29, 2010*. 2010, MIT.
5. George, M.W., *Selenium and Tellurium*, in *Mineral Year Book*. 2013, U. S. Geologic Survey.
6. Goldfarb, R.J., et al., *Tellurium- Economic and Environmental Geology, and Prospects for Future Supply*. 2014.

7.   Zweibel, K., *The impact of tellurium supply on cadmium telluride photovoltaics.* Science, 2010. **328**(5979): p. 699-701.

8.   Houari, Y., et al., *A system dynamic model of tellurium availability for CdTe PV.* Progress in Photovoltaics: Research and Applications, 2014. **22**: p. 129-146.

9.   Green, M.A., *Estimates of Te and In prices from direct mining of known ores.* Progress in Photovoltaics, 2009. **17**(5): p. 347-359.

10.   Fthenakis, V., W.M. Wang, and H.C. Kim, *Life cycle inventory analysis of the production of metals used in photovoltaics.* Renewable & Sustainable Energy Reviews, 2009. **13**(3): p. 493-517.

11.   Ojebuoboh, F., *Selenium and tellurium from copper refinery slimes and their changing applications.* World of Metallurgy, 2008. **61**(1): p. 33-39.

12.   Marsden, J. and I. House, *The Chemistry of Gold Extraction.* 2006, Englewood, CO: Society for Mining, Metallurgy, and Exploration, Inc.

13.   Chizhikov, D.M. and V.P. Shchasttlivyi, *Tellurium and Tellurides.* 1970, London: Collet's Publishers.

14.   Tremblay, J.-F., *Managing a dearth of rare earths.* Chemical and Engineering News, 2012: p. 14.

15.   Harada, T. and Y. Takahashi, *Origin of the difference in the distribution behavior of tellurium and selenium in a soil-water system.* Geochimica et Cosmochimica Acta, 2009. **72**(5): p. 1281-1294.

16.   NREL. *Solar Research.* 2014; Available from: http://www.nrel.gov/ncpv/images/efficiency_chart.jpg.

17.   Solar, F. *First Solar.* 2014 [cited 2014 October 26]; Available from: http://www.firstsolar.com.

18.   DiSalvo, F.J., *Thermoelectric cooling and power generation.* Science, 1999. **285**(5428): p. 703-706.

19.   Goldschmid, H.J. and R.W. Douglas, *The use of semiconductors in thermoelectric refrigeration.* British Journal of Applied Physics, 1954. **5**: p. 386-390.

20.   Dughaish, Z.H., *Lead telluride as a thermoelectric material for thermoelectric power generation.* Physica B-Condensed Matter, 2002. **322**(1-2): p. 205-223.

21.   Li, J.F., et al., *High-performance nanostructured thermoelectric materials.* Npg Asia Materials, 2010. **2**(4): p. 152-158.

22.   Ravich, Y.I., B.A. Efimova, and I.A. Smirnov, *Semiconducting Lead Chalcogenides.* 1970, New York: Plenum Press.

23.   Heikes, R.R. and R.W. Ure, *Thermoelectricity: Science and Engineering.* 1961, New York: Interscience Publishers.

24.   Gelbstein, Y., Z. Dashevsky, and M.P. Dariel, *High performance n-type PbTe-based materials for thermoelectric applications.* Physica B-Condensed Matter, 2005. **363**(1-4): p. 196-205.

25.   Jingwen, M., C. Yuchuan, and W. Ping'An, *Geology and geochemistry of the Dashuigou tellurium deposit, western Sichuan, China.* International Geology Review, 1995. **37**: p. 526-546.

26.   Dunken, H.H., *Mining for gold in Fiji-4, operation of the Emperor Gold Mining, Co. Ltd. at Vatukoula, Colony, of Fiji.* Australian Mining, 1969. **61**: p. 33-43.

27.   New Boliden, *Metals for modern life.*, 2013. http://www.bergforsk.se/wp-content/uploads/2013/06/marklund_boliden.pdf.

28. Jensen, E.P. and M.D. Barton, *Gold deposits related to alkaline magmatism*, in *Gold in 2000: Reviews in Economic Geology*, 2000. p. 279-314.

29. Saunders, J.A. and M.E. Brueske, *Volatility of Se and Te during subduction-related distillation and the geochemistry of epithermal ores of the western United States.* Economic Geology, 2012. **117**: p. 165-172.

30. Everett, F.D., *Reconnaissance of tellurium resources in Arizona, Colorado, New Mexico and Utah.* 1964, Department of the Interior, Bureau of Mines.

31. Boyle, R.W., *The geochemistry of Gold and its Deposits.* 1979, Geological Survey of Canada, Bulletin. p. 584.

32. Titley, S.R. and R.E. Beane, *Porphyry copper deposits, Part I. Geologic settings, petrology, and tectogenesis*, in *Economic Geology 75th Anniversary Volume*, B.J. Skinner, Editor. 1981. p. 214-235.

33. Cox, L.J., et al., *Porphyry Cu deposits.* 1995, U.S. Geological Survey. p. Ch. 11, 15

34. Seedorff, E., et al., *Porphyry deposits: Characteristics and origin of hypogene features*, in *Economic Geology 100th Anniversary Volume*, J.W. Hedenquist, et al., Editors. 2005. p. 251-298.

35. Gott, G.B. and J.H. McCarthy, *Distribution of gold, silver, tellurium, and mercury in the Ely mining district, White Pine County, Nevada.* 1966, U.S. Geological Survey Circular 535. p. 1-5.

36. Einaudi, M.T., L.D. Meinert, and R.J. Newberry, *Skarn deposits*, in *Economic Geology 75th Anniversary Volume*, B.J. Skinner, Editor. 1981, Economic Geology. p. 317-391.

37. Einaudi, M.T. and D.M. Burt, *Introduction—Terminology, classification, and composition of skarn deposits.* Economic Geology, 1982. **77**: p. 745-754.

38. Einaudi, M.T., *Skarns associated with porphyry copper deposits: description of deposits; I Southwestern North America, II General features and origin*, in *Advances in the geology of the porphyry copper deposits, southwestern North America*, S.R. Titley, Editor. 1982, University of Arizona Press: Tucson, AZ.

39. Pals, D.W. and P.G. Spry, *Telluride mineralogy of the low-sulfidation epithermal Emperor gold deposit, Vatukoula, Fiji.* Mineralogy and Petrology, 2003. **79**(3-4): p. 285-307.

40. Scherbarth, N.L. and P.G. Spry, *Mineralogical, petrological, stable isotope, and fluid inclusion characteristics of the Tuvatu gold-silver telluride deposit, Fiji: Comparisons with the Emperor deposit.* Economic Geology, 2006. **101**(1): p. 135-158.

41. Spry, P.G., et al., *The mineralogy of the Golden Sunlight gold-silver telluride deposit, Whitehall, Montana, USA.* Mineralogy and Petrology, 1997. **59**(3-4): p. 143-164.

42. Zhang, X.M. and P.G. Spry, *Petrological, mineralogical, fluid inclusion, and stable-Isotope studies of the Gies gold-silver telluride deposit, Judith Mountains, Montana.* Economic Geology, 1994. **89**(3): p. 602-627.

43. Cocker, M.D., *Primary element dispersion patterns in a carbonate-hosted, epithermal, high-grade, Au-Ag telluride system- Mayflower mine, Madison County, Montana, USA.* Journal of Geochemical Exploration, 1993. **47**(1-3): p. 377-390.

44. Deditus, A., et al., *Trace metal nanoparticles in pyrite.* Ore Geology Reviews 2011. **42**: p. 32-46.

45. Large, R.R., et al., *Gold and trace element zonation in pyrite using a laser imaging technique: Implications for timing of gold in orogenic and Carlin-style sediment-hosted deposits.* Economic Geology, 2009. **104**: p. 635-668.

46. Morey, A.A., et al., *Bimodal distribution of gold in pyrite and arsenopyrite: Examples from the Archean Boorara and Bardoc shear systems, Yilgarn Craton, Western Australia.* Economic Geology, 2005. **103**: p. 599-614.

47. Paktunc, D., et al., *Distribution of gold in pyrite and in products of its transformation resulting from roasting of refractory gold ore.* Canadian Mineralogist, 2006. **44** (1): p. 213-227.

48. Pals, D.W., P.G. Spry, and S. Chryssoulis, *Invisible gold and tellurium in arsenic-rich pyrite from the Emperor gold deposit, Fiji: Implications for gold distribution and deposition.* Economic Geology, 2003. **98**(3): p. 479-493.

49. Spry, P.G., S. Chryssoulis, and C.G. Ryan, *Process mineralogy of gold: Gold telluride-bearing ores.* Journal of Metals, 2004. **August**: p. 62-65.

50. Bogdanov, K., A. Filipov, and I. Kehayov, *Au-Ag-Te-Se minerals in the Elatsite porphyry-copper deposit, Bulgaria*, in *Au-Ag-Te-Se deposits, IGCP project 486, 2005 field workshop, Kiten, Bulgaria 14-19 September 2005*. 2005: Bulgarian Academy of Sciences, Geochemistry, Mineralogy, and Petrology. p. 13-20.

51. Maglambayan, V.B., et al., *Geology, mineralogy, and formation environment of the disseminated gold-silver telluride Bulawan deposit, Negros Occidental, Philippines.* Resource Geology, 1998. **48**(2): p. 87-104.

52. Eliopoulos, D.G., M. Economou-Eliopoulos, and M. Zelyaskova-Panayiotova, *Critical factors controlling Pd and Pt potential in porphyry Cu–Au deposits: Evidence from the Balkan Peninsula.* Geoscience, 2014. **4**: p. 31-49.

53. Eaton, P.C. and T.N. Setterfield, *The relationship between epithermal and porphyry hydrothermal systems within the Tavua Caldera, Fiji.* Economic Geology, 1993. **88**: p. 1053-1083.

54. Fornadel, A.P., et al., *Methods for the determination of stable Te isotopes of minerals in the system Au-Ag-Te by MC-ICP-MS.* Journal of Analytical Atomic Spectrometry, 2014. **29**(4): p. 623-637.

55. Voudouris, P., et al., *Rhenium-rich molybdenite and rheniite (ReS2) in the Pagoni Rachi-Kirki Mo-Cu-Te-Ag-Au deposit, northern Greece: Implications for the rhenium geochemistry of porphyry style Cu-Mo and Mo mineralization.* Canadian Mineralogist, 2009. **47**: p. 1013-1036.

56. Yano, R.I., *Trace element distribution in chalcopyrite-bearing porphyry and skarn deposits*. M.S. thesis. 2012, University of Nevada, Reno, 103 p.

57. Kase, K., *Tellurian tennantite from the Besshi-type deposits in the Sanbagawa metamorphic belt, Japan.* Canadian Mineralogist, 1986. **29**: p. 399-404.

58. Reich, M., et al., *Solubility of gold in arsenian pyrite.* Geochimica et Cosmochimica Acta, 2005. **69**(11): p. 2781-2796.

59. Schlesinger, M.E., et al., *Extractive Metallurgy of Copper*. 5th ed. 2011, New York: Elsevier.

60.   Moats, M., et al., *Electrolytic copper refining? 2007 tankhouse operating data.* Proceedings of the Sixth International Copper-Cobre Conference, Toronto, Ontario, Canada, 2007: p. 195-242.

61.   Chen, T.T. and J.E. Dutrizac, *Mineralogical characterization of anode slimes. 6. Pressure leached slimes from the CCR Division of Noranda Minerals Inc.* Canadian Metallurgical Quarterly, 1990. **29**(4): p. 293-305.

62.   Chen, T.T. and J.E. Dutrizac, *The mineralogical characterization of tellurium in copper anodes.* Metallurgical Transactions B-Process Metallurgy, 1993. **24**(6): p. 997-1007.

63.   Chen, T.T. and J.E. Dutrizac, *Mineralogical characterization of anode slimes. 10. Tellurium in raw anode slimes.* Canadian Metallurgical Quarterly, 1996. **35**(4): p. 337-351.

64.   Chen, T.T. and J.E. Dutrizac, *The deportment of selenium and tellurium during the electrorefining of copper*, in *Minor elements 2000: Processing and environmental aspects of As, Sb, Se, Te, and Bi.*, C.M. Young, Editor. 2000, Society of Mining, Metallurgy, and Exploration, Inc: Littleton, CO. p. 199-212.

65.   Brookins, D.G., *Eh-pH Diagrams for Geochemistry.* 1988, Berlin: Springer-Verlag.

66.   Grundler, P.V., et al., *Speciation of aqueous tellurium (IV) in hydrothermal solutions and vapors, and the role of oxidized tellurium species in Te transport and gold deposition.* Geochimica et Cosmochimica Acta, 2013. **120:** p. 298-325.

67.   Taylor, A. *Biochemistry of Tellurium.* in *New perspectives in the research of hardly known trace elements and in element interaction.* 1994. Budapest: University of Horticulture and Food Science.

68.   Meza-Figueroa, D., et al., *The impact of unconfined mine tailings in residential areas from a mining town in a semi-arid environment: Nacozari, Sonora, Mexico.* Chemosphere, 2009. **77**(1): p. 140-147.

69.   Hayes, S.M., et al., *Geochemical weathering increases lead bioaccessibility in semi-arid mine tailings.* Environmental Science and Technology, 2012. **46**(11): p. 5834-5841.

70.   Csavina, J., et al., *A review on the importance of metals and metalloids in atmospheric dust and aerosol from mining operations.* Science of the Total Environment, 2013. **433**: p. 58-73.

71.   Breshears, D.D., et al., *Wind and water erosion and transport in semi-arid shrubland, grassland and forest ecosystems: Quantifying dominance of horizontal wind-driven transport.* Earth Surface Processes and Landforms, 2003. **28**(11): p. 1189-1209.

72.   Derry, L.A. and O.A. Chadwick, *Contributions from Earth's atmosphere to soil.* Elements, 2007. **3**(5): p. 333-338.

73.   Kim, C.S., D.H. Stack, and J.J. Rytuba, *Fluvial transport and surface enrichment of arsenic in semi-arid mining regions: examples from the Mojave Desert, California.* Journal of Environmental Monitoring, 2012. **14**(7): p. 1798-1813.

74.   Kron, T., C. Hansen, and E. Werner, *Renal excretion of tellurium after peroral administration of tellurium in different forms to healthy human volunteers.* Journal of Trace Elements and Electrolytes in Health and Disease., 1991. **5**: p. 239-244.

75.   Plumlee, G.S., T.L. Ziegler, and B.S. Lollar, *The medical geochemistry of dusts, soils, and other earth materials*, in *Environmental Geochemistry*, H.D. Holland and K.K. Turekian, Editors. 2005, Elsevier: Amsterdam. p. 263-310.

76.   Schaider, L.A., et al., *Characterization of zinc, lead, and cadmium in mine waste: Implications for transport, exposure, and bioavailability.* Environmental Science & Technology, 2007. **41**(11): p. 4164-4171.

77.   Kashiwabara, T., et al., *Chemical processes for the extreme enrichment of tellurium into marine ferromanganese oxides.* Geochimica et Cosmochimica Acta, 2014. **131**: p. 150-163.

78.   Grundler, P.V., et al., *Xocolatlite, $Ca_2Mn_2^{4+}Te_2O_{12}.H_2O$, a new tellurate related to kuranakhite: Description and measurement of Te oxidation state by XANES spectroscopy.* American Mineralogist, 2008. **93**(11-12): p. 1911-1920.

79.   Brugger, J., et al., *XAS evidence for the stability of polytellurides in hydrothermal fluids up to 599 degrees C, 800 bar.* American Mineralogist, 2012. **97**(8-9): p. 1519-1522.

80.   ASARCO. *ASARCO, Groupo Mexico.* 2014; Available from: http://www.asarco.com.

81.   Argall, G.D., *ASARCO's Mission Copper. Mining World.* Engineering & Mining Journal 1962. **24**(1): p. 19-24.

82.   *Barrick.* 2015; Available from: http://www.barrick.com/operations/united-states/golden-sunlight/default.aspx

83.   Spry, P.G. and S.E. Thieben, *The distribution and recovery of gold in the Golden Sunlight gold-silver telluride deposit, Montana, USA.* Mineralogical Magazine, 2000. **64**(1): p. 31-42.

84.   Meisel, T., *Determination of rare earth elements, Y, Th, Zr, Hf, Nb, and Ta in geological reference materials G-2, G-3, SCo-1 and WGB-1 by sodium peroxide sintering and inductively coupled plasma mass spectrometry.* Geostandards Newsletter - Journal of Geostandards and Geoanalysis, 2002. **26**(1): p. 53-61.

85.   Hayes, S.M., et al., *Surficial weathering of iron sulfide mine tailings under semi-arid climate.* Geochimica et Cosmochimica Acta, 2014. **141**: p. 240-257.

86.   Webb, S.M., *Sixpack: A graphical user interface for XAS analysis using IFEFFIT.* Physica Scripta, 2005. **T115**: p. 1011-1014.

87.   Csavina, J., et al., *A review on the importance of metals and metalloids in atmospheric dust and aerosol from mining operations.* Science of the Total Environment, 2012. **433**: p. 58-73.

88.   Hoffman, J., *Recovering selenium and tellurium from copper refinery slimes.* Journal of Minerals, Metals and Materials Society, 1989. **41**(7): p. 33-38.

89.   Porter, E.W. and E. Ripley, *Petrologic and stable isotope study of the gold-bearing breccia pipe at the Golden Sunlight deposit, Montana.* Economic Geology, 1985. **80**(6): p. 1689-1706.

90.   Thieben, S.E. and P.G. Spry, *The geology and geochemistry of Cretaceous-Tertiary alkaline igneous rock-related gold-silver telluride deposits of Montana, USA*, ed. J. Pasava, B. Kribek, and K. Zak. 1995, Rotterdam, Netherlands: A.A. Balkema, Rotterdam.

91.	Kyle, J.H., et al., *Review of trace toxic elements (Pb, Cd, Hg, As, Sb, Bi, Se, Te) and their deportment in gold processing. Part 1: Mineralogy, aqueous chemistry and toxicity.* Hydrometallurgy, 2011. **107**(3-4): p. 91-100.

92.	Deschenes, G., et al., *Kinetics and mechanism of leaching synthetic calaverite in cyanide solutions.* Minerals and Metallurgical Processing, 2006. **23**(3): p. 133-138.

93.	Kyle, J.H., et al., *Review of trace toxic elements (Pb, Cd, Hg, As, Sb, Bi, Se, Te) and their deportment in gold processing: Part II: Deportment in gold ore processing by cyanidation.* Hydrometallurgy, 2012. **111-112**: p. 10-21.

94.	Paredes, M., *A fluid inclusion, stable isotope, and multi-element study of the Golden Sunlight deposit, Montana*, in *Geological and Atmospheric Sciences*. 1994, Iowa State University: Ames, IA. p. 174.

95.	Root, R.A., S.M. Hayes, and J. Chorover, *Investigation of contaminant metal lability and speciation with depth in mine tailings from the Iron King Superfund Site.* Applied Geochemistry, 2015. **62**: p. 131-149.

96.	Hein, J.R., A. Koschinsky, and A.N. Halliday, *Global occurrence of tellurium-rich ferromanganese crusts and a model for the enrichment of tellurium.* Geochimica et Cosmochimica Acta, 2003. **67**(6): p. 1117-1127.